Studying Atmospheric Neutrino Oscillations with PINGU

2014.09.11 at UW Madison

Kaoru Hagiwara

KEK Theory Center and Sokendai

Three neutrino model has 9 parameters:

3 masses	m_1, m_2, m_3
3 angles	θ_{23}, θ_{12}, θ_{13}
3 phases	δ_{MNS}, α_1, α_2

Neutrino oscillation experiments can measure 6 out of the 9 parameters:

2 mass-squared differences	$m_2^2 - m_1^2$, $m_3^2 - m_1^2$
3 angles	θ_{23}, θ_{12}, θ_{13}
1 phase	δ_{MNS}

Both mass-squared differences and **ALL** 3 angles have been measured. The tasks of the future neutrino oscillation experiments are to determine:

the mass hierarchy	$m_3^2 - m_1^2 > 0$ or $m_3^2 - m_1^2 < 0$
the octant degeneracy	$\theta_{23} < \pi/4$ or $\theta_{23} > \pi/4$
the CP phase	δ_{MNS}

besides sharpening of the existing measurements and search for new physics.

Recent works of my colleagues on possible neutrino oscillation experiments in the near future include:

- Reactor anti-neutrino at DayaBayII(JUNO), RENO50,
  - · medium baseline 50 km$< L <$60 km
  - · lower energy 1 MeV$< E <$8 MeV.

  S.F.Ge, KH, N.Okamura, Y.Takaesu, [arXiv:1210.8241] JHEP 1305(2013)131

- Accelerator neutrino
  - · long baselines:
    T2K(T2HK) (L =295 km), Tokai-to-Oki (L =653 km),
    NOνA (L =812 km), Tokai-to-Korea (L =1000 km),
    LBNE (L =1300 km), LBNO (L =2300 km), ...
  - · medium energy 0.5 GeV$< E <$5 GeV.

  KH, T.Kiwanami, N.Okamura, K.Senda, [arXiv:1209.2763] JHEP 1306(2013)036
  KH, P.Ko, N.Okamura, Y.Takaesu, in preparation.

- Atmospheric neutrino SK(HK), INO, PINGU
  - · very long baseline a few $\times$ 1000 km$< L <$13000 km
  - · high energies 2 GeV$< E <$20 GeV.

  S.F.Ge, KH, C.Rott, [arXiv:1309.3176] JHEP 06(2014)150
  S.F.Ge, KH, [arXiv:1312.0457] JHEP 09(2014)024

In this talk, I would like to show that dedicated studies on Atmospheric Neutrino Oscillations by a huge detector like **PINGU** in ICECUBE can determine the neutrino mass hierarchy and resolve the octant degeneracy in θ_{23}, the two of the three remaining unkowns of the 3 neutrino model parameters. The measurement of the CP phase δ is significantly more challenging.

The talk is based on the following two papers:

- *A Novel Approach to Study Atmospheric Neutrino Oscillation*
  S.F. Ge, KH, C. Rott, [arXiv:1309.3176v3] JHEP 06(2014)150

- *Physics Reach of Atmospheric Neutrino Measurements at PINGU*
  S.F. Ge and KH, [arXiv:1312.0457v3] JHEP 09(2014)024

In the first paper, a novel analysis framework of neutrino oscillation in the matter is proposed, in which the earth matter effects as well as the dependences on the mixing angles θ_{12} and θ_{13} of the oscillation probabilities are factorized into several coefficients of the analytically known dependeces on θ_{23} and δ.

In the second paper, we applied the framework to conduct a semi-realistic simulation of **PINGU** measurements, by treating the neutrino scattering kinematics exactly for both charged and neutral currents and by adopting a primitive detector simulation with energy and angular resolutions of muonic and cascade signals. The robustness of the **PINGU** measurements in the presence of several systematic errors and their combinations has also been demonstrated in the second paper.

A novel approach to study atmospheric neutrino oscillation

Shao-Feng Ge,[a] **Kaoru Hagiwara**[b] **and Carsten Rott**[c]

[a] *KEK Theory Center, Tsukuba, 305-0801, Japan*

[b] *KEK Theory Center and Sokendai, Tsukuba, 305-0801, Japan*

[c] *Department of Physics, Sungkyunkwan University, Suwon 440-746, Korea*

E-mail: gesf02@gmail.com, kaoru.hagiwara@kek.jp, carsten.rott@gmail.com

Abstract: We develop a general theoretical framework to analytically disentangle the contributions of the neutrino mass hierarchy, the atmospheric mixing angle, and the CP phase, in neutrino oscillations. To illustrate the usefulness of this framework, especially that it can serve as a complementary tool to neutrino oscillogram in the study of atmospheric neutrino oscillations, we take PINGU as an example and compute muon- and electron-like event rates with event cuts on neutrino energy and zenith angle. Under the assumption of exact measurement of neutrino momentum with a perfect e-μ identification and no background, we find that the PINGU experiment has the potential of resolving the neutrino mass hierarchy and the octant degeneracies within 1-year run, while the measurement of the CP phase is significantly more challenging. Our observation merits a serious study of the detector capability of estimating the neutrino momentum for both muon- and electron-like events.

JHEP06(2014)150

PREM

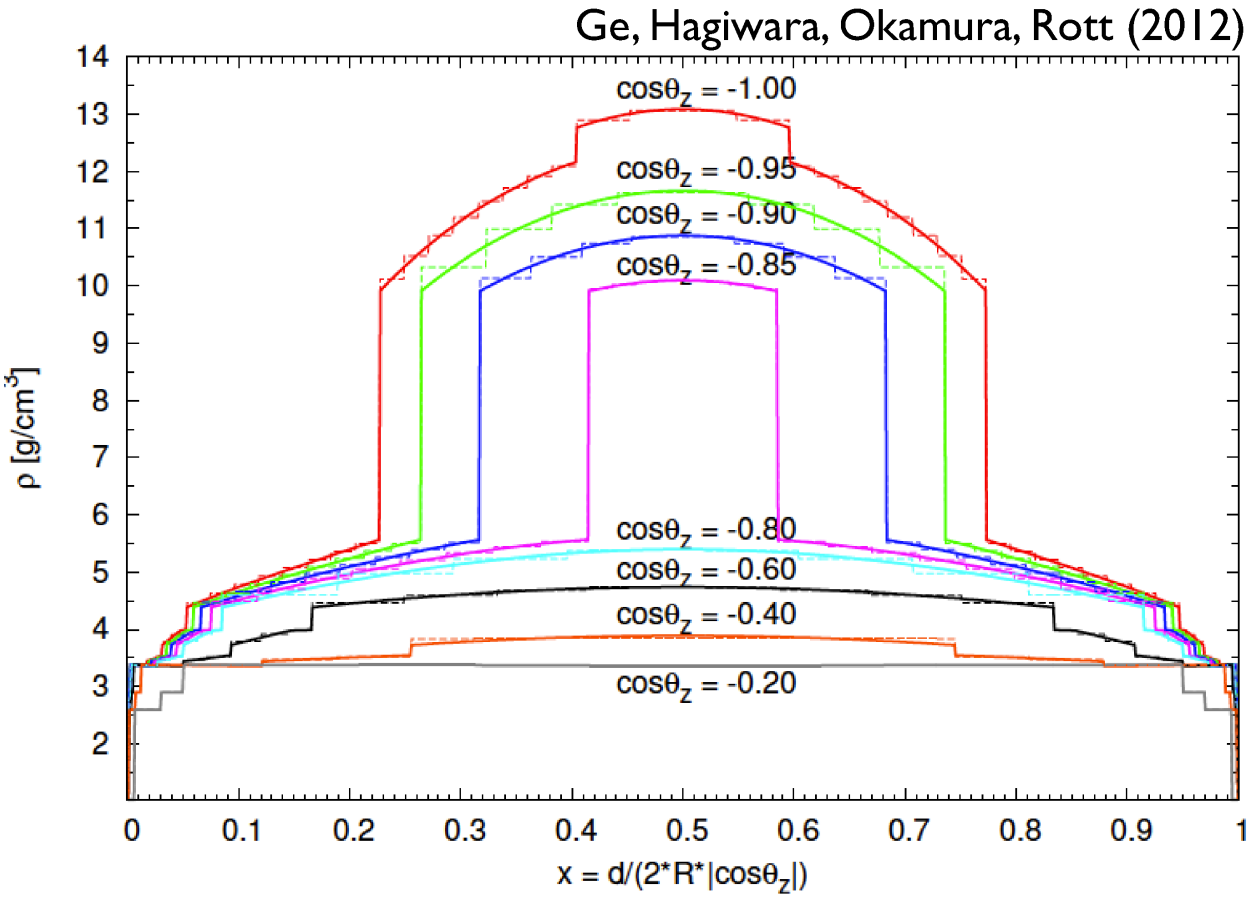

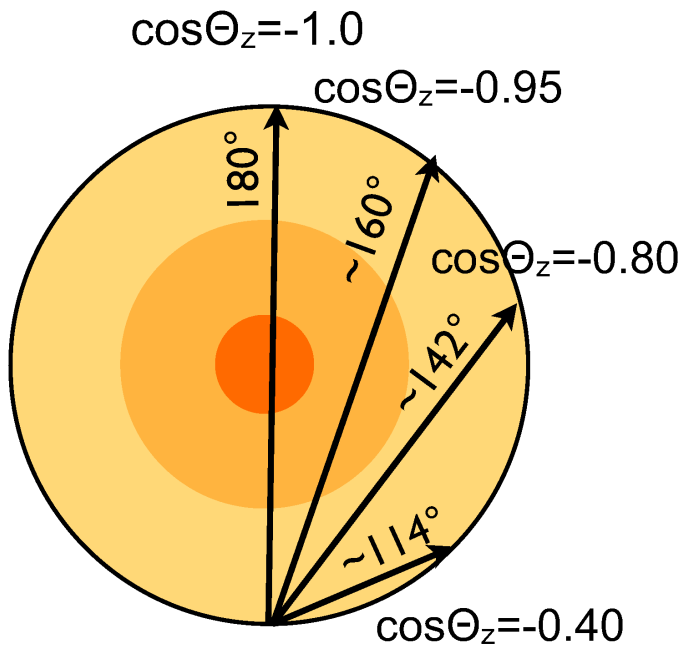

- The PREM - Preliminary Reference Earth Model is based on a paper by Dziewonski and Anderson in 1981. It still still represents the standard framework for interpretation of seismological data

3.1. Propagation Basis

$$\mathcal{H} = \frac{1}{2E_\nu}\left[U\begin{pmatrix}0 & & \\ & \delta m_s^2 & \\ & & \delta m_a^2\end{pmatrix}U^\dagger + \begin{pmatrix}a(x) & & \\ & 0 & \\ & & 0\end{pmatrix}\right], \tag{3.1}$$

where $a(x) \equiv 2E_\nu V(x) = 2\sqrt{2}E_\nu G_F N_e(x)$ characterizes the matter effect, $\delta m_s^2 \equiv \delta m_{12}^2$ & $\delta m_a^2 \equiv \delta m_{13}^2$,

$$U \equiv O_{23}(\theta_a)P_\delta O_{13}(\theta_r)P_\delta^\dagger O_{12}(\theta_s) = \begin{pmatrix}1 & & \\ & c_a & s_a \\ & -s_a & c_a\end{pmatrix}\begin{pmatrix}1 & & \\ & 1 & \\ & & e^{i\delta}\end{pmatrix}\begin{pmatrix}c_r & & s_r \\ & 1 & \\ -s_r & & c_r\end{pmatrix}\begin{pmatrix}1 & & \\ & 1 & \\ & & e^{-i\delta}\end{pmatrix}\begin{pmatrix}c_s & s_s & \\ -s_s & c_s & \\ & & 1\end{pmatrix},$$

where $c_\alpha \equiv \cos\theta_\alpha$ and $s_\alpha \equiv \sin\theta_\alpha$ with $(s, a, r) \equiv (12, 23, 13)$. Note that in this basis O_{23} and P_δ can be extracted out as overall matrices [42],

$$\mathcal{H} = \frac{1}{2E_\nu}(O_{23}P_\delta)\left[(O_{13}O_{12})\begin{pmatrix}0 & & \\ & \delta m_s^2 & \\ & & \delta m_a^2\end{pmatrix}(O_{13}O_{12})^\dagger + \begin{pmatrix}a(x) & & \\ & 0 & \\ & & 0\end{pmatrix}\right](O_{23}P_\delta)^\dagger. \tag{3.2}$$

This is a huge simplification,

$$\mathcal{H}' = \frac{1}{2E_\nu}\left[(O_{13}O_{12})\begin{pmatrix}0 & & \\ & \delta m_s^2 & \\ & & \delta m_a^2\end{pmatrix}(O_{13}O_{12})^\dagger + \begin{pmatrix}a(x) & & \\ & 0 & \\ & & 0\end{pmatrix}\right] = (O_{23}P_\delta)^\dagger\mathcal{H}(O_{23}P_\delta). \tag{3.3}$$

Propagation Basis

$$\nu_\alpha = [O_{23}(\theta_a)P_\delta]_{\alpha i}\nu'_i. \tag{3.4}$$

$$S = (O_{23}P_\delta)S'(O_{23}P_\delta)^\dagger \equiv (O_{23}P_\delta)\begin{pmatrix}S'_{11} & S'_{12} & S'_{13} \\ S'_{21} & S'_{22} & S'_{23} \\ S'_{31} & S'_{32} & S'_{33}\end{pmatrix}(O_{23}P_\delta)^\dagger, \tag{3.5}$$

with $S'_{ij} \equiv \langle\nu'_j|S'|\nu'_i\rangle$ and $S_{\beta\alpha} \equiv \langle\nu_\beta|S|\nu_\alpha\rangle$.

3.2. Oscillation Probabilities

$$
\begin{aligned}
S_{ee} &= S'_{11}\,, && (3.14a)\\
S_{e\mu} &= c_a S'_{12} + s_a e^{-i\delta} S'_{13}\,, && (3.14b)\\
S_{\mu e} &= c_a S'_{21} + s_a e^{+i\delta} S'_{31}\,, && (3.14c)\\
S_{\mu\mu} &= c_a^2 S'_{22} + c_a s_a (e^{-i\delta} S'_{23} + e^{+i\delta} S'_{32}) + s_a^2 S'_{33}\,. && (3.14d)
\end{aligned}
$$

Note that only the elements among e and μ flavors are shown since they are sufficient to derive all the flavor basis oscillation probabilities, $P_{\alpha\beta} \equiv P(\nu_\alpha \to \nu_\beta) = |\langle \nu_\beta | S | \nu_\alpha \rangle|^2 = |S_{\beta\alpha}|^2$,

$$
\begin{aligned}
P_{ee} \equiv |S_{ee}|^2 &= |S'_{11}|^2\,, && (3.15a)\\
P_{e\mu} \equiv |S_{\mu e}|^2 &= c_a^2\,|S'_{12}|^2 + s_a^2\,|S'_{13}|^2 + 2c_a\,s_a\,(\cos\delta\,\mathbb{R} + \sin\delta\,\mathbb{I})(S'_{12}\,S'^{*}_{13})\,, && (3.15b)\\
P_{\mu e} \equiv |S_{e\mu}|^2 &= c_a^2\,|S'_{21}|^2 + s_a^2\,|S'_{31}|^2 + 2c_a\,s_a\,(\cos\delta\,\mathbb{R} - \sin\delta\,\mathbb{I})(S'_{21}\,S'^{*}_{31})\,, && (3.15c)\\
P_{\mu\mu} \equiv |S_{\mu\mu}|^2 &= c_a^4\,|S'_{22}|^2 + s_a^4\,|S'_{33}|^2 + 4c_a^2\,s_a^2\,\mathbb{R}\,(S'_{22}\,S'^{*}_{33})\\
&+ c_a^2\,s_a^2\,\left[|S'_{23}|^2 + 2(\cos 2\delta\,\mathbb{R} + \sin 2\delta\,\mathbb{I})(S'_{23}\,S'^{*}_{32}) + |S'_{32}|^2\right]\\
&+ 2\,c_a\,s_a\,\cos\delta\,\mathbb{R}[(c_a^2\,S'_{22} + s_a^2\,S'_{33})(S'_{23} + S'_{32})^*]\\
&+ 2\,c_a\,s_a\,\sin\delta\,\mathbb{I}[(c_a^2\,S'_{22} + s_a^2\,S'_{33})(S'_{32} - S'_{23})^*]\,, && (3.15d)
\end{aligned}
$$

where $\mathbb{R}$ and $\mathbb{I}$ gives the real and imaginary parts, respectively. The transition probability into ν_τ are then obtained by unitarity conditions, $P_{e\tau} = 1 - P_{ee} - P_{e\mu}$, $P_{\mu\tau} = 1 - P_{\mu e} - P_{\mu\mu}$, $\overline{P}_{\alpha\beta} \equiv P(\bar\nu_\alpha \to \bar\nu_\beta) = P_{\alpha\beta}(a(x) \to -a(x), \delta \to -\delta)$,

3.3. Simplifications with Symmetric Matter Profile

The oscillation amplitude matrix after experiencing a reversible matter profile is symmetric in the absence of CP violation [45].

$$
S'_{ij} = S'_{ji}\,. \qquad (3.16)
$$

2.4. Expansion of Oscillation Probabilities with respect to $x_{\rm a} = \cos 2\theta_{\rm a}$ and $\delta m^2_{\rm s}$

The deviation of θ_a from its maximal value $\theta_a = \frac{\pi}{4}$ can be explored analytically,

$$c^2_{\rm a} = \frac{1}{2}(1 + x_{\rm a})\,, \qquad s^2_{\rm a} = \frac{1}{2}(1 - x_{\rm a})\,, \qquad c^2_{\rm a} s^2_{\rm a} = \frac{1}{4}(1 - x^2_{\rm a})\,. \tag{2.22}$$

Then,

$$P_{\alpha\beta} \equiv P^{(0)}_{\alpha\beta} + P^{(1)}_{\alpha\beta} x_{\rm a} + P^{(2)}_{\alpha\beta} \cos\delta' + P^{(3)}_{\alpha\beta} \sin\delta' + P^{(4)}_{\alpha\beta} x_{\rm a} \cos\delta' + P^{(5)}_{\alpha\beta} x^2_{\rm a} + P^{(6)}_{\alpha\beta} \cos^2\delta'\,, \tag{2.23a}$$

$$\overline{P}_{\alpha\beta} \equiv \overline{P}^{(0)}_{\alpha\beta} + \overline{P}^{(1)}_{\alpha\beta} x_{\rm a} + \overline{P}^{(2)}_{\alpha\beta} \cos\delta' + \overline{P}^{(3)}_{\alpha\beta} \sin\delta' + \overline{P}^{(4)}_{\alpha\beta} x_{\rm a} \cos\delta' + \overline{P}^{(5)}_{\alpha\beta} x^2_{\rm a} + \overline{P}^{(6)}_{\alpha\beta} \cos^2\delta'\,, \tag{2.23b}$$

with $\cos\delta' \equiv 2c_a s_a \cos\delta = \sqrt{1 - x^2_a}\cos\delta$, $\sin\delta' \equiv 2c_a s_a \sin\delta = \sqrt{1 - x^2_a}\sin\delta$.

	$P^{(k)}_{\rm ee}$	$P^{(k)}_{{\rm e}\mu}$	$P^{(k)}_{\mu{\rm e}}$	$P^{(k)}_{\mu\mu}$
(0)	$\lvert S'_{11}\rvert^2$	$\frac{1}{2}(1 - \lvert S'_{11}\rvert^2)$	$\frac{1}{2}(1 - \lvert S'_{11}\rvert^2)$	$\frac{1}{4}\lvert S'_{22} + S'_{33}\rvert^2$
(1)	0	$\frac{1}{2}(\lvert S'_{12}\rvert^2 - \lvert S'_{13}\rvert^2)$	$\frac{1}{2}(\lvert S'_{12}\rvert^2 - \lvert S'_{13}\rvert^2)$	$\frac{1}{2}(\lvert S'_{22}\rvert^2 - \lvert S'_{33}\rvert^2)$
(2)	0	$\mathbb{R}(S'_{12} S'^*_{13})$	$\mathbb{R}(S'_{12} S'^*_{13})$	$\mathbb{R}[S'_{23}(S'_{22} + S'_{33})^*]$
(3)	0	$\mathbb{I}(S'_{12} S'^*_{13})$	$-\mathbb{I}(S'_{12} S'^*_{13})$	0
(4)	0	0	0	$\mathbb{R}[S'_{23}(S'_{22} - S'_{33})^*]$
(5)	0	0	0	$\frac{1}{4}\lvert S'_{22} - S'_{33}\rvert^2$
(6)	0	0	0	$\lvert S'_{23}\rvert^2$

(2.24)

$$S'_{12} \sim S'_{23} \sim \delta m^2_s / \delta m^2_a \sim 3\%$$

$$\mathcal{H}' = \frac{1}{2E_\nu}\left[(O_{13}O_{12})\begin{pmatrix} 0 & & \\ & \delta m^2_s & \\ & & \delta m^2_a \end{pmatrix}(O_{13}O_{12})^\dagger + \begin{pmatrix} a(x) & & \\ & 0 & \\ & & 0 \end{pmatrix}\right] = (O_{23}P_\delta)^\dagger \mathcal{H} (O_{23}P_\delta)\,. \tag{3.4}$$

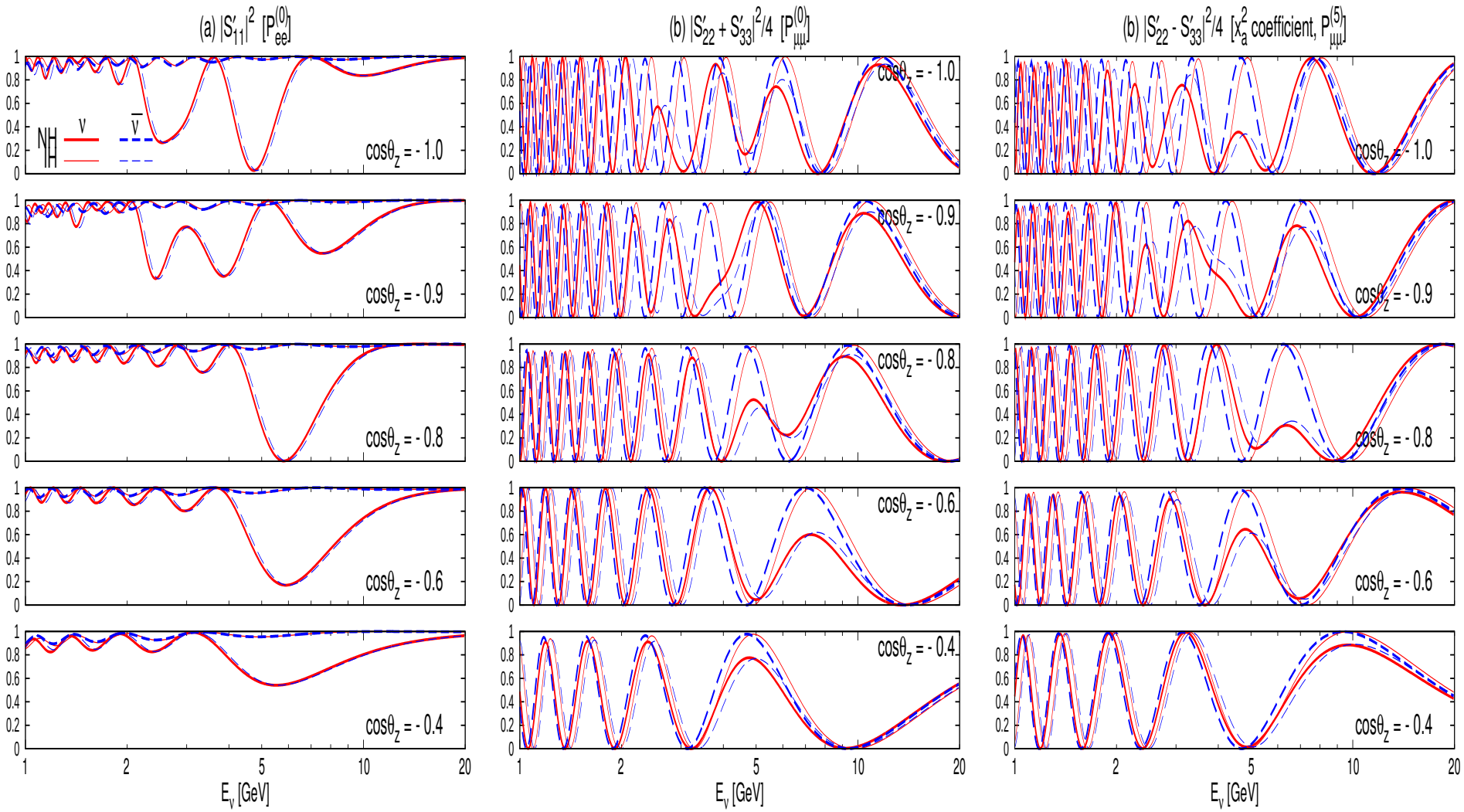

	$P^{(k)}_{ee}$	$P^{(k)}_{e\mu}$	$P^{(k)}_{\mu e}$	$P^{(k)}_{\mu\mu}$
(0)	$\lvert S'_{11}\rvert^2$	$\frac{1}{2}(1-\lvert S'_{11}\rvert^2)$	$\frac{1}{2}(1-\lvert S'_{11}\rvert^2)$	$\frac{1}{4}\lvert S'_{22}+S'_{33}\rvert^2$
(1) x_a	0	$-\frac{1}{2}(1-\lvert S'_{11}\rvert^2)$	$-\frac{1}{2}(1-\lvert S'_{11}\rvert^2)$	$\frac{1}{2}(1-\lvert S'_{11}\rvert^2)$
(5) x_a^2	0	0	0	$\frac{1}{4}\lvert S'_{22}-S'_{33}\rvert^2$

(2.32)

Oscillogram

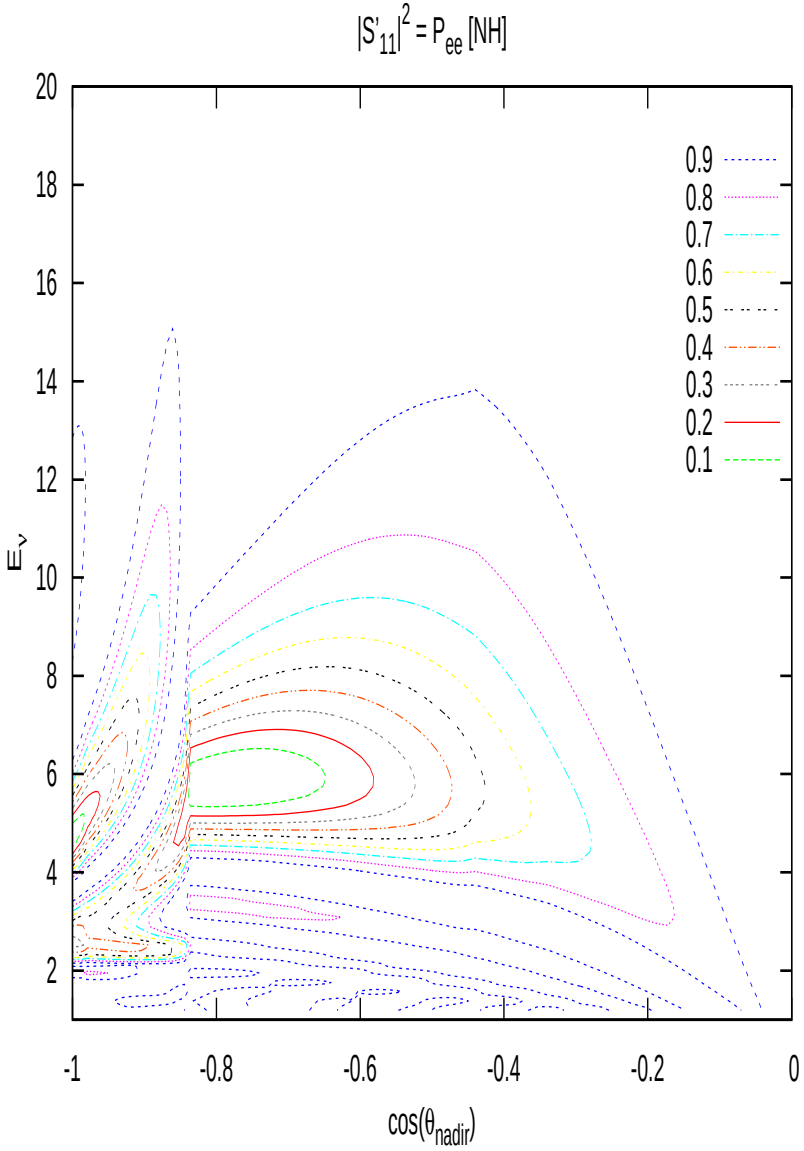

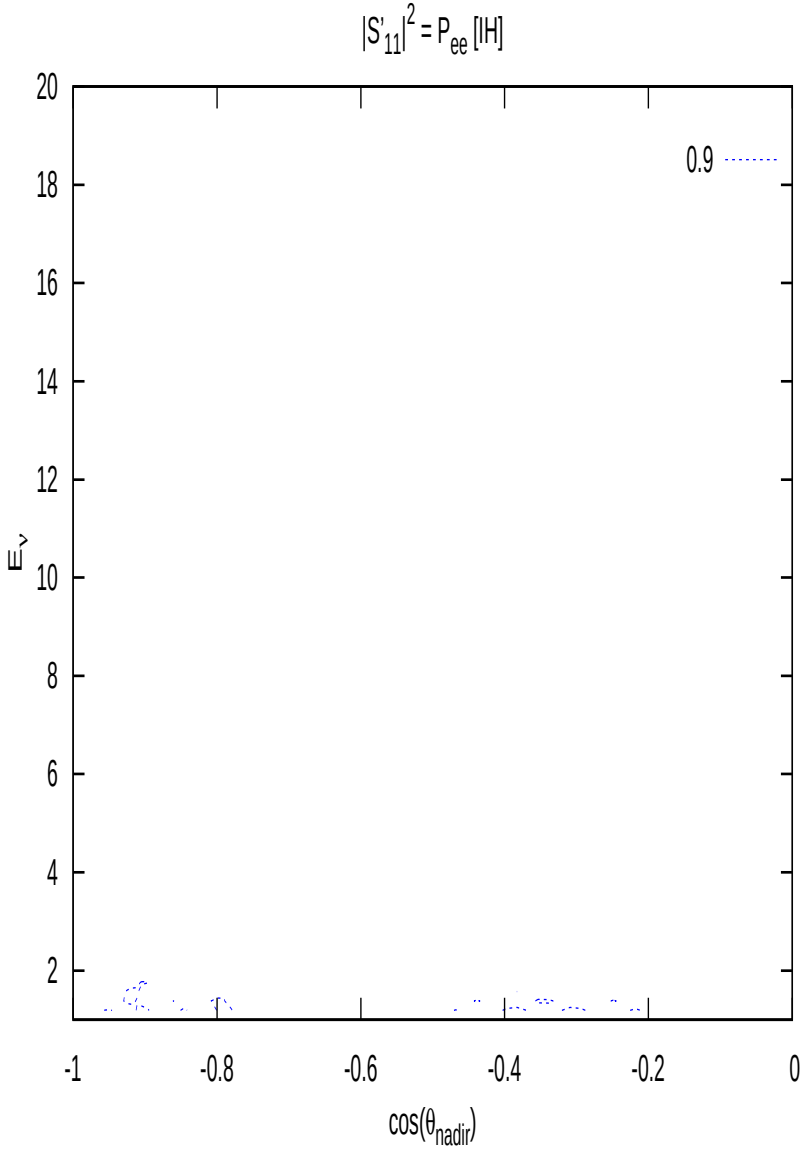

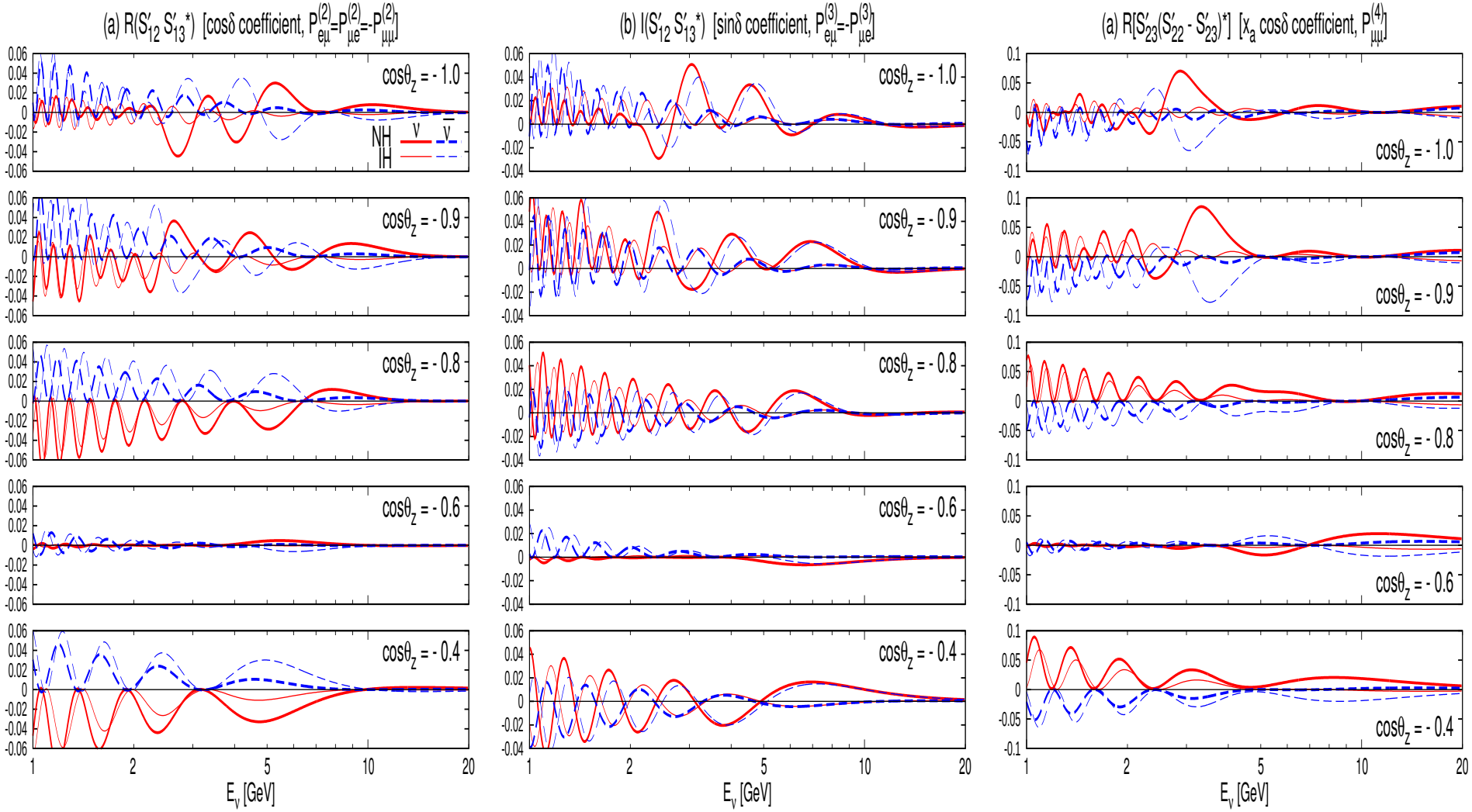

	$P^{(k)}_{\rm ee}$	$P^{(k)}_{\rm e\mu}$	$P^{(k)}_{\mu\rm e}$	$P^{(k)}_{\mu\mu}$
(2) $\cos\delta'$	0	$\mathbb{R}(S'_{12}S'^{*}_{13})$	$\mathbb{R}(S'_{12}S'^{*}_{13})$	$-\mathbb{R}(S'_{12}S'^{*}_{13})$
(3) $\sin\delta'$	0	$\mathbb{I}(S'_{12}S'^{*}_{13})$	$-\mathbb{I}(S'_{12}S'^{*}_{13})$	0
(4) $x_a\cos\delta'$	0	0	0	$\mathbb{R}[S'_{23}(S'_{22}-S'_{33})^{*}]$

(2.32)

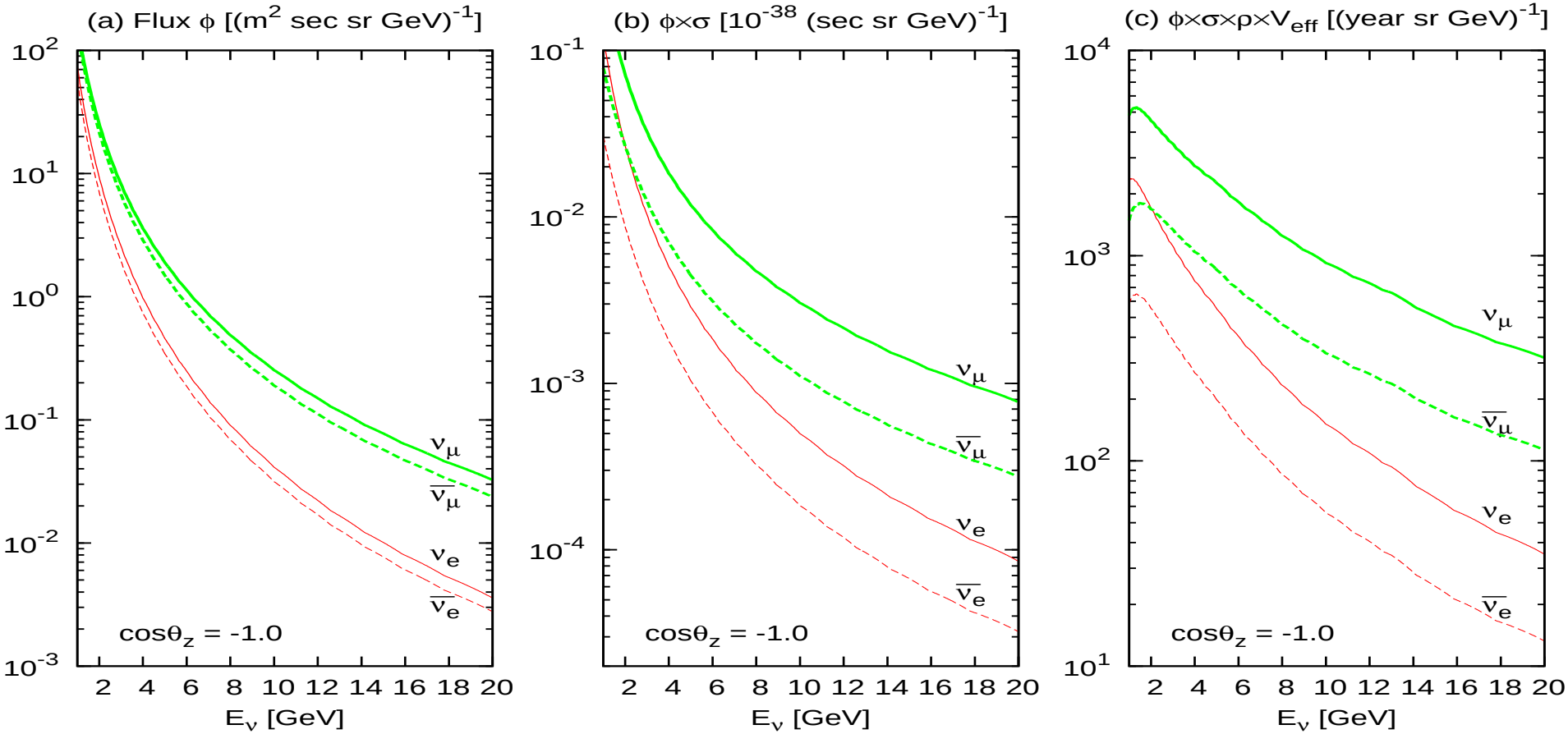

$$\frac{dN_{\rm e}}{dE_\nu d\cos\theta_{\rm z}} = \big\{[\phi_{\nu_{\rm e}}(E_\nu,\cos\theta_{\rm z})P_{\rm ee}(E_\nu,\cos\theta_{\rm z})+\phi_{\nu_\mu}(E_\nu,\cos\theta_{\rm z})P_{\mu{\rm e}}(E_\nu,\cos\theta_{\rm z})]\sigma_{\nu_{\rm e}}(E_\nu)$$
$$+[\phi_{\bar\nu_{\rm e}}(E_\nu,\cos\theta_{\rm z})\overline{P}_{\rm ee}(E_\nu,\cos\theta_{\rm z})+\phi_{\bar\nu_\mu}(E_\nu,\cos\theta_{\rm z})\overline{P}_{\mu{\rm e}}(E_\nu,\cos\theta_{\rm z})]\sigma_{\bar\nu_{\rm e}}(E_\nu)\big\}\,\rho V_{\rm eff}(E_\nu)\,, \quad (3.1a)$$

$$\frac{dN_\mu}{dE_\nu d\cos\theta_{\rm z}} = \big\{[\phi_{\nu_{\rm e}}(E_\nu,\cos\theta_{\rm z})P_{{\rm e}\mu}(E_\nu,\cos\theta_{\rm z})+\phi_{\nu_\mu}(E_\nu,\cos\theta_{\rm z})P_{\mu\mu}(E_\nu,\cos\theta_{\rm z})]\sigma_{\nu_\mu}(E_\nu)$$
$$+[\phi_{\bar\nu_{\rm e}}(E_\nu,\cos\theta_{\rm z})\overline{P}_{{\rm e}\mu}(E_\nu,\cos\theta_{\rm z})+\phi_{\bar\nu_\mu}(E_\nu,\cos\theta_{\rm z})\overline{P}_{\mu\mu}(E_\nu,\cos\theta_{\rm z})]\sigma_{\bar\nu_\mu}(E_\nu)\big\}\,\rho V_{\rm eff}(E_\nu)\,, \quad (3.1b)$$

Since the event rates depend on the oscillation probabilities linearly, they can also be decomposed accordingly,

$$\frac{dN_\alpha}{dE_\nu d\cos\theta_{\rm z}} \equiv N_\alpha^{(0)} + N_\alpha^{(1)}x_{\rm a} + N_\alpha^{(2)}\cos\delta' + N_\alpha^{(3)}\sin\delta' + N_\alpha^{(4)}x_{\rm a}\cos\delta' + N_\alpha^{(5)}x_{\rm a}^2 + N_\alpha^{(6)}\cos^2\delta'\,. \quad (3.2)$$

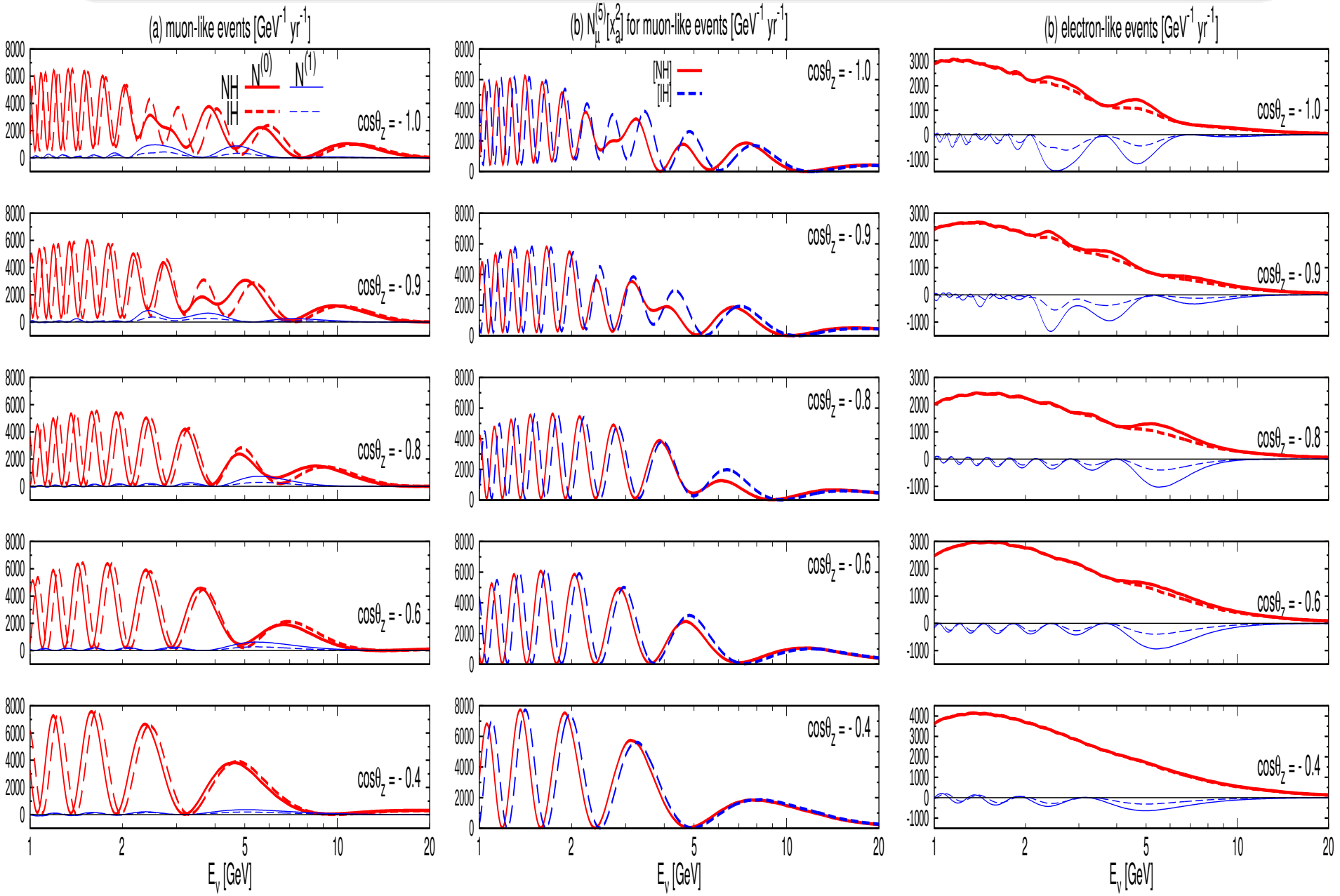
(a) muon-like events [GeV^{-1} yr^{-1}]
(b) $N_\mu^{(5)}[x_a^2]$ for muon-like events [GeV^{-1} yr^{-1}]
(b) electron-like events [GeV^{-1} yr^{-1}]
NH
IH
$N^{(0)}$
$N^{(1)}$
[NH]
[IH]
$\cos\theta_z = -1.0$
$\cos\theta_z = -0.9$
$\cos\theta_z = -0.8$
$\cos\theta_z = -0.6$
$\cos\theta_z = -0.4$
E_ν [GeV]

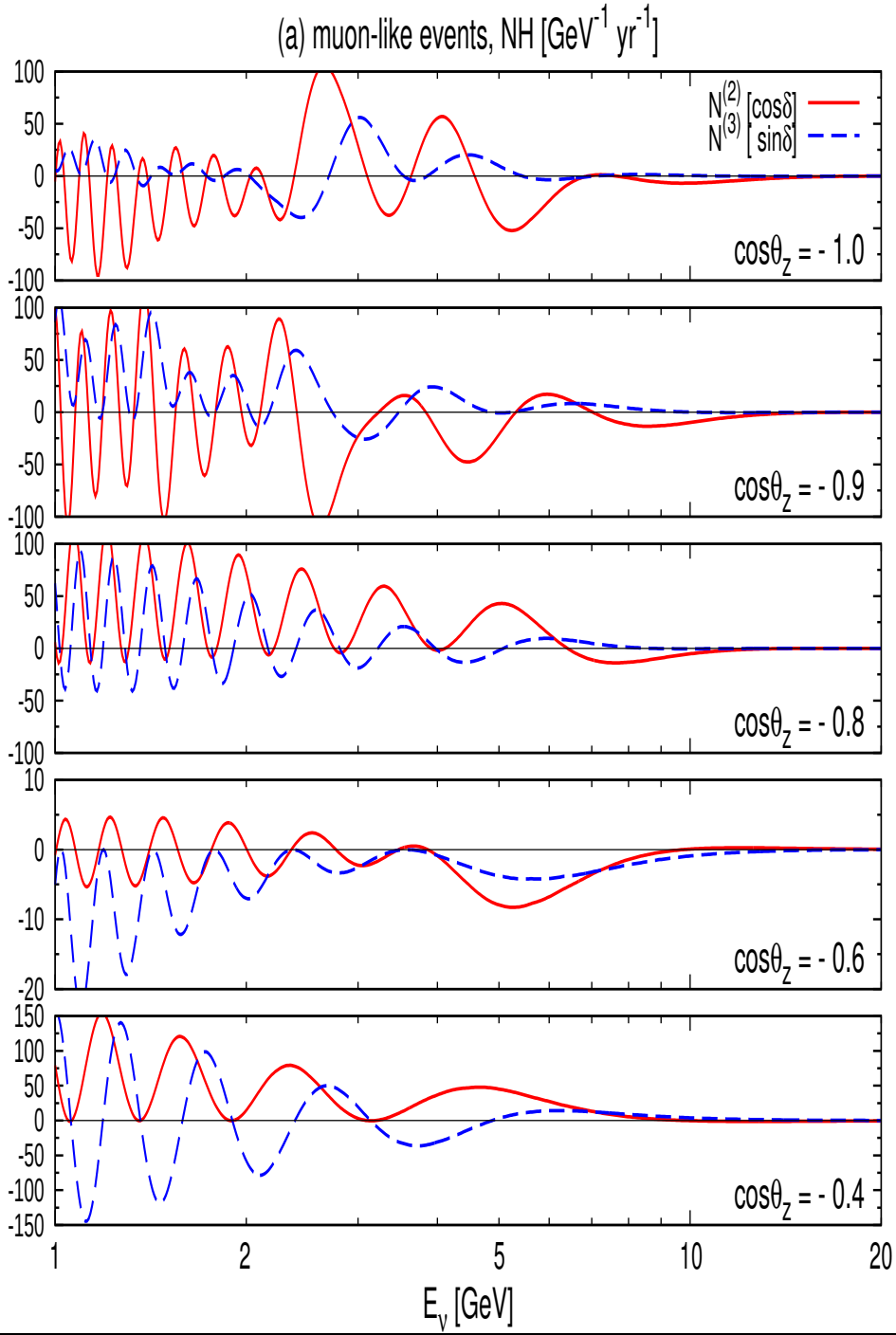
(a) muon-like events, NH [GeV^{-1} yr^{-1}]
$N^{(2)}$ [cosδ]
$N^{(3)}$ [sinδ]
cosθ$_z$ = - 1.0
cosθ$_z$ = - 0.9
cosθ$_z$ = - 0.8
cosθ$_z$ = - 0.6
cosθ$_z$ = - 0.4
E$_\nu$ [GeV]

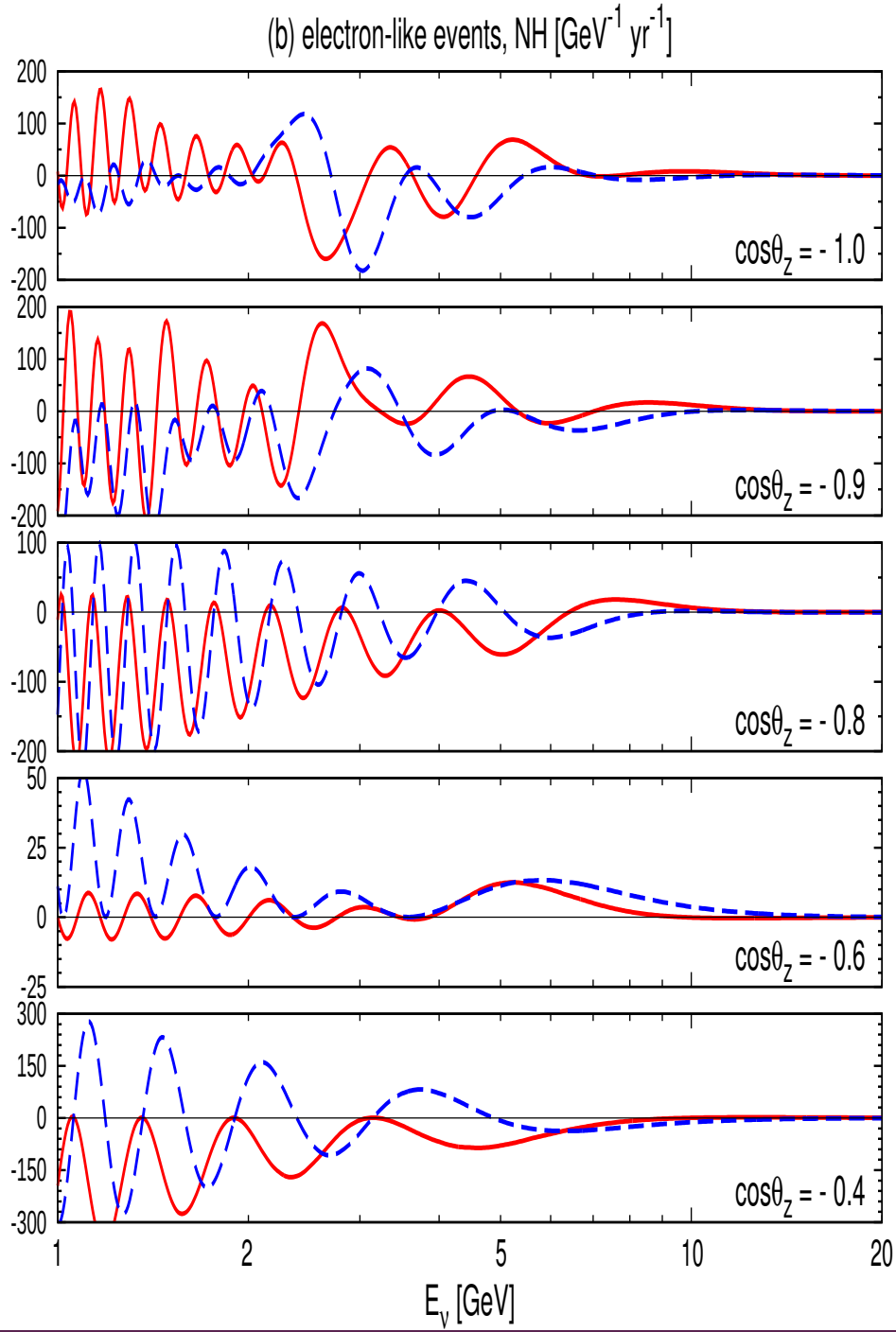
(b) electron-like events, NH [GeV^{-1} yr^{-1}]
cosθ$_z$ = - 1.0
cosθ$_z$ = - 0.9
cosθ$_z$ = - 0.8
cosθ$_z$ = - 0.6
cosθ$_z$ = - 0.4
E$_\nu$ [GeV]

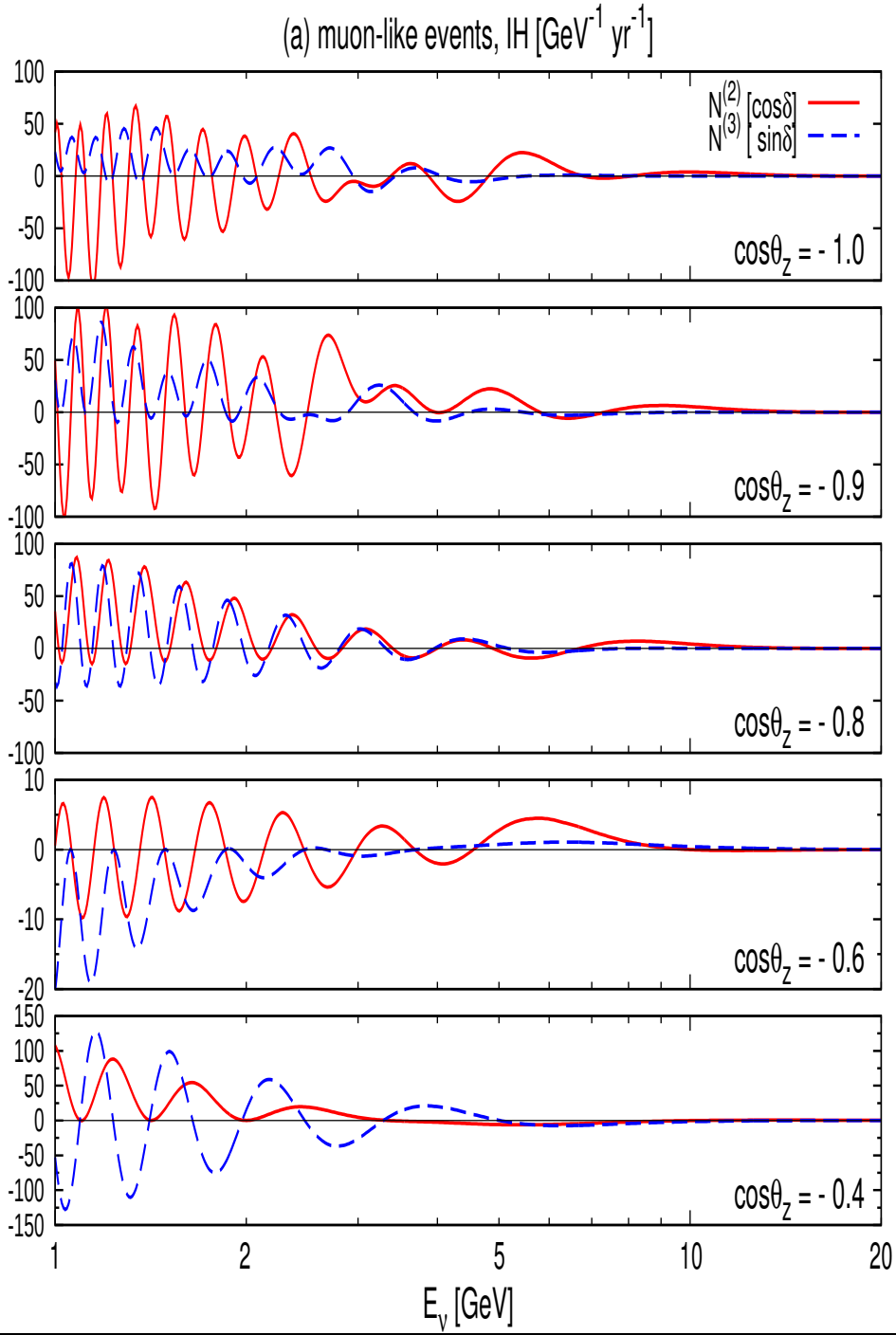
(a) muon-like events, IH [GeV^{-1} yr^{-1}]
$N^{(2)}$ [cosδ]
$N^{(3)}$ [sinδ]
cosθ$_z$ = - 1.0
cosθ$_z$ = - 0.9
cosθ$_z$ = - 0.8
cosθ$_z$ = - 0.6
cosθ$_z$ = - 0.4
E$_\nu$ [GeV]

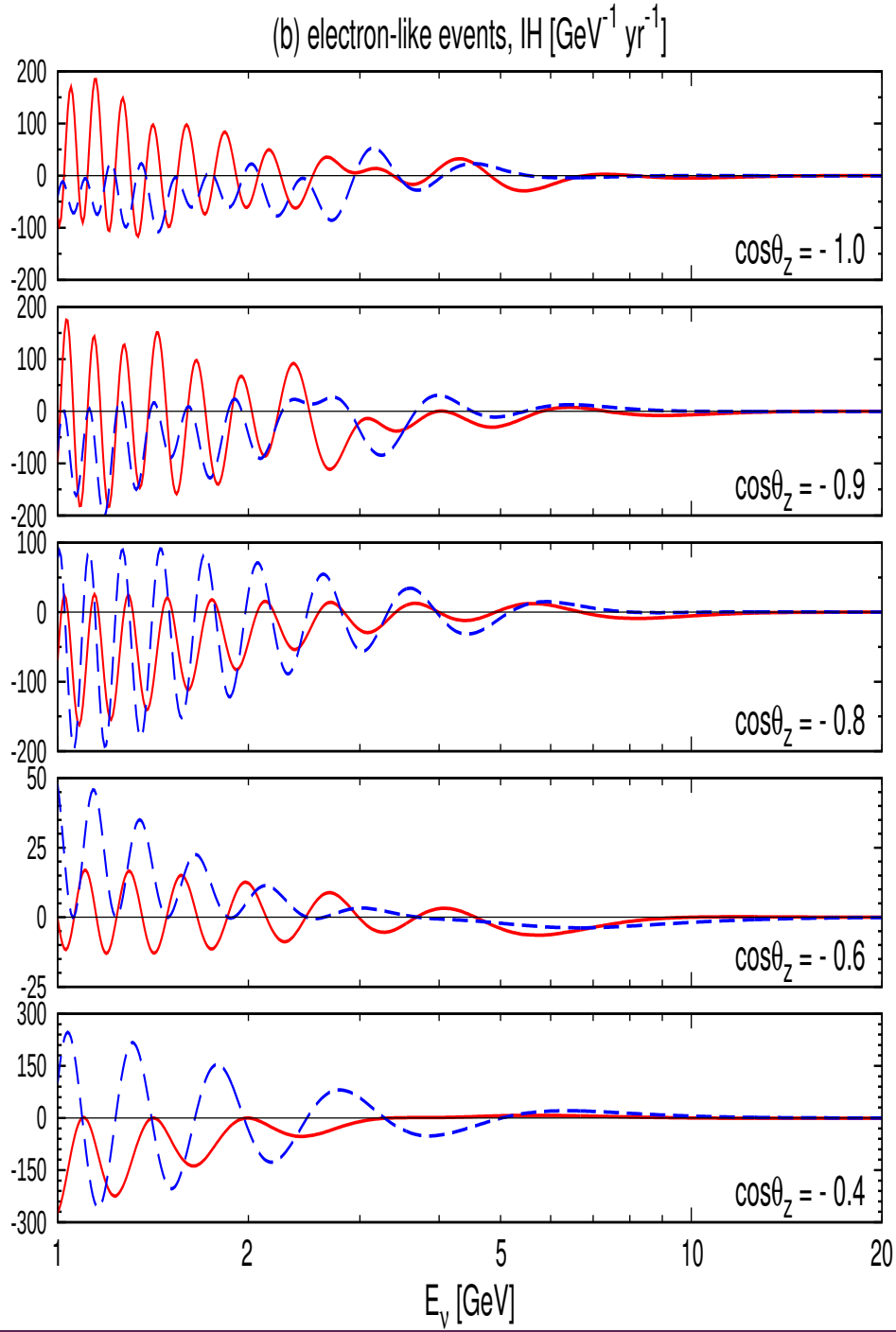
(b) electron-like events, IH [GeV^{-1} yr^{-1}]
cosθ$_z$ = - 1.0
cosθ$_z$ = - 0.9
cosθ$_z$ = - 0.8
cosθ$_z$ = - 0.6
cosθ$_z$ = - 0.4
E$_\nu$ [GeV]

Physics reach of atmospheric neutrino measurements at PINGU

Shao-Feng Ge[a] **and Kaoru Hagiwara**[b]

[a] *KEK Theory Center, Tsukuba, 305-0801, Japan*

[b] *KEK Theory Center and Sokendai, Tsukuba, 305-0801, Japan*

E-mail: gesf02@gmail.com, kaoru.hagiwara@kek.jp

Abstract: The sensitivity of a huge underground water/ice Cherenkov detector, such as PINGU in IceCube, to the neutrino mass hierarchy, the atmospheric mixing angle and its octant, is studied in detail. Based on the event rate decomposition in the propagation basis, we illustrate the smearing effects from the neutrino scattering, the visible energy and zenith angle reconstruction procedures, the energy and angular resolutions, and the muon mis-identification rate, as well as the impacts of systematic errors in the detector resolutions, the muon mis-identification rate, and the overall normalization. The sensitivity, especially the mass hierarchy sensitivity, can be enhanced by splitting the muon-like events into two channels, according to the event inelasticity. We also show that including the cascade events can improve and stabilize the sensitivity of the measurements.

JHEP09(2014)024

Sample Reconstructed Events

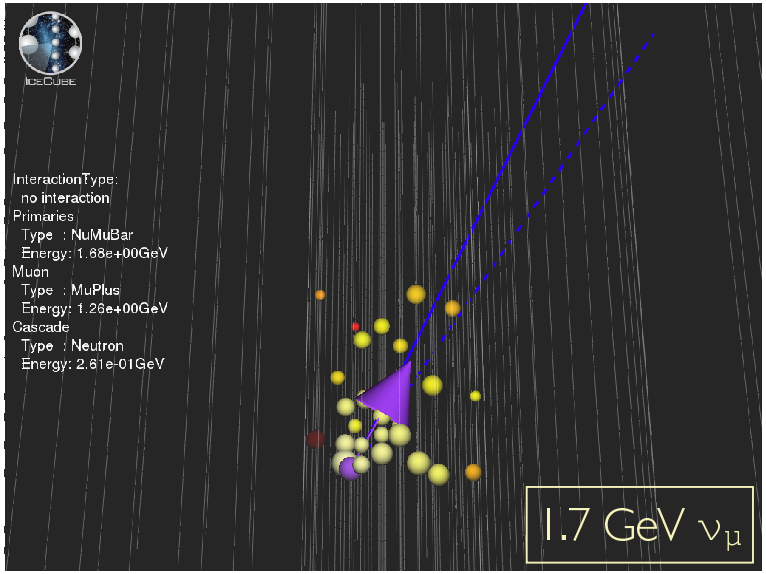

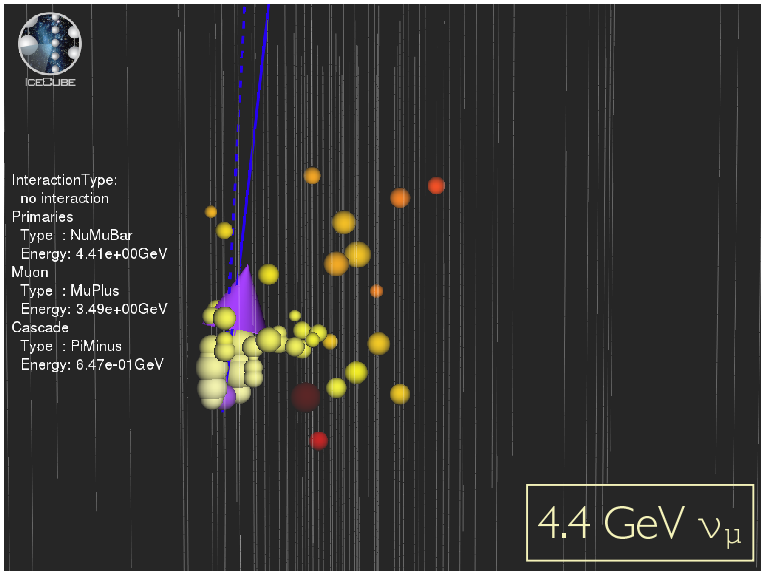

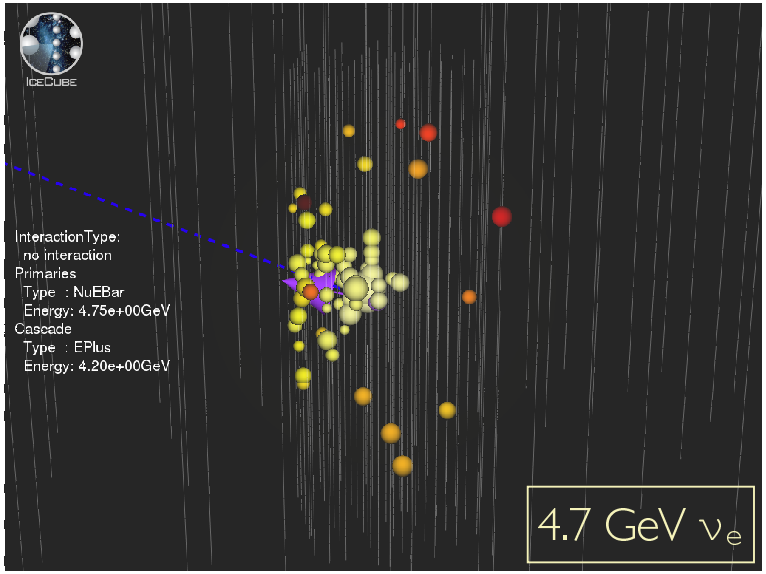

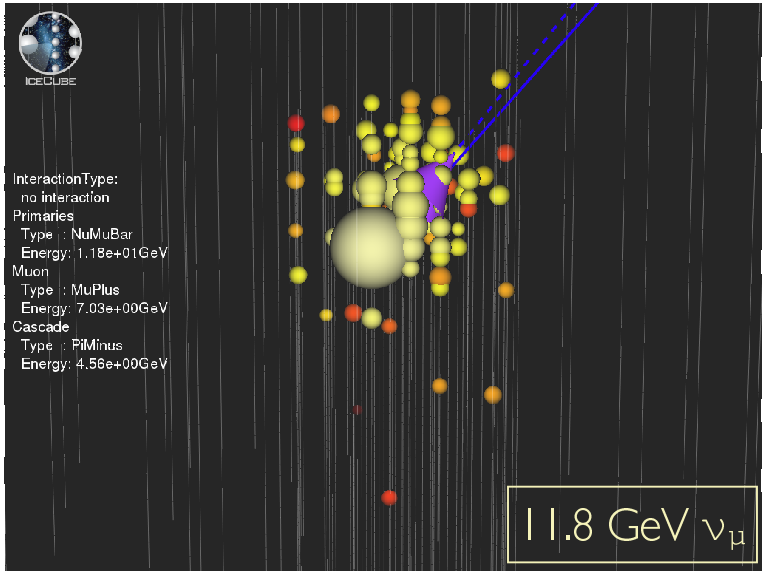

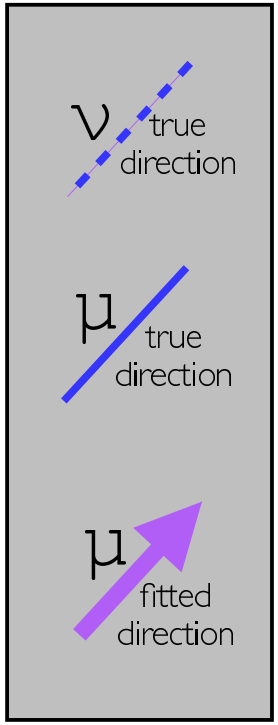

Size of circles: N_γ.
Color: t_γ.

$$E_{\rm cas} \equiv 0.8 \times (E_\nu - E_{\nu'} - E_\ell) + E_{\rm e}\,, \tag{3.4}$$

where E_ν and $E_{\nu'}$ are the energies of the incident and the final-state neutrinos, respectively. For μ-CC and e-CC, $E_{\nu'} = 0$ and it can be large for NC and τ-CC events. For μ-CC events, $E_\ell = E_\mu$ and $E_{\rm e} = 0$, while for e-CC events, $E_\ell = E_{\rm e}$.

There are two typical topologies on PINGU. Muon with large enough energy, $E_\mu > 1\,\text{GeV}$, leaves a clear track due to its long lifetime while the cascade produced by other particles has a spherical structure. Because of this difference, the energies of muon and cascade can be reconstructed independently. This distinguishability makes estimating the muon inelasticity possible, as defined in (3.3). On the other hand, the electron shower cannot be distinguished from cascade, hence, its energy cannot be measured separately. For muon with small energy, $E_\mu < 1\,\text{GeV}$, the track may not be long and clear enough to be identified, and it is counted as cascade events. In addition, 10% of the energetic muons, $E_\mu > 1\,\text{GeV}$, are assumed to be mis-identified as cascade events [43]. For τ, it decays very quickly into muon, electron, or hadrons. For all these cases, the visible energy can then be estimated as,

$$E_{\rm vis} \equiv E_\mu + \frac{E_{\rm cas}}{0.8} = \begin{cases} E_\nu & \mu - CC\,(E_\mu > 1\,\text{GeV with 90\% } \mu\text{-ID})\,, \\ E_\nu + 0.25E_{\ell'} & \begin{cases} e - CC\,, \\ \mu - CC\,(E_\mu < 1\,\text{GeV}, E_\mu > 1\,\text{GeV with 10\% } \mu\text{-misID})\,, \end{cases} \\ E_\nu - E_{\nu'} & \begin{cases} \tau - CC \text{ with } \tau \to \mu\,(E_\mu > 1\,\text{GeV with 90\% } \mu\text{-ID})\,, \\ \tau - CC \text{ with } \tau \to \text{hadrons}\,, \\ NC\,, \end{cases} \\ E_\nu - E_{\nu'} + 0.25E_{\ell'} & \tau - CC \begin{cases} \tau \to e\,, \\ \tau \to \mu\,(E_\mu < 1\,\text{GeV}, E_\mu > 1\,\text{GeV with 10\% } \mu\text{-misID})\,, \end{cases} \end{cases} \tag{3.5}$$

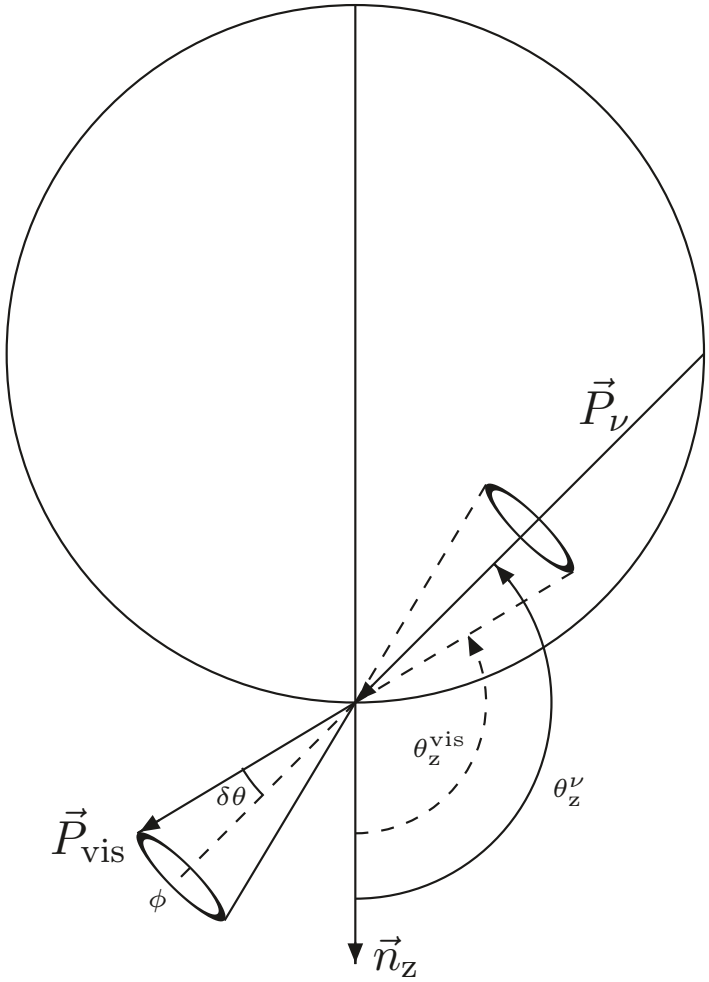

Figure 3. Kinematics of neutrino scattering.

expressed as,

$$\vec{P}_{\rm vis} = \begin{cases} \vec{P}_\ell & CC\,(E_\ell > 1\,\mathrm{GeV})\,, \\ \vec{P}_\nu - \vec{P}_{\nu'} & \begin{cases} CC\,(E_\ell < 1\,\mathrm{GeV})\,, \\ NC\,, \end{cases} \end{cases} \tag{3.6}$$

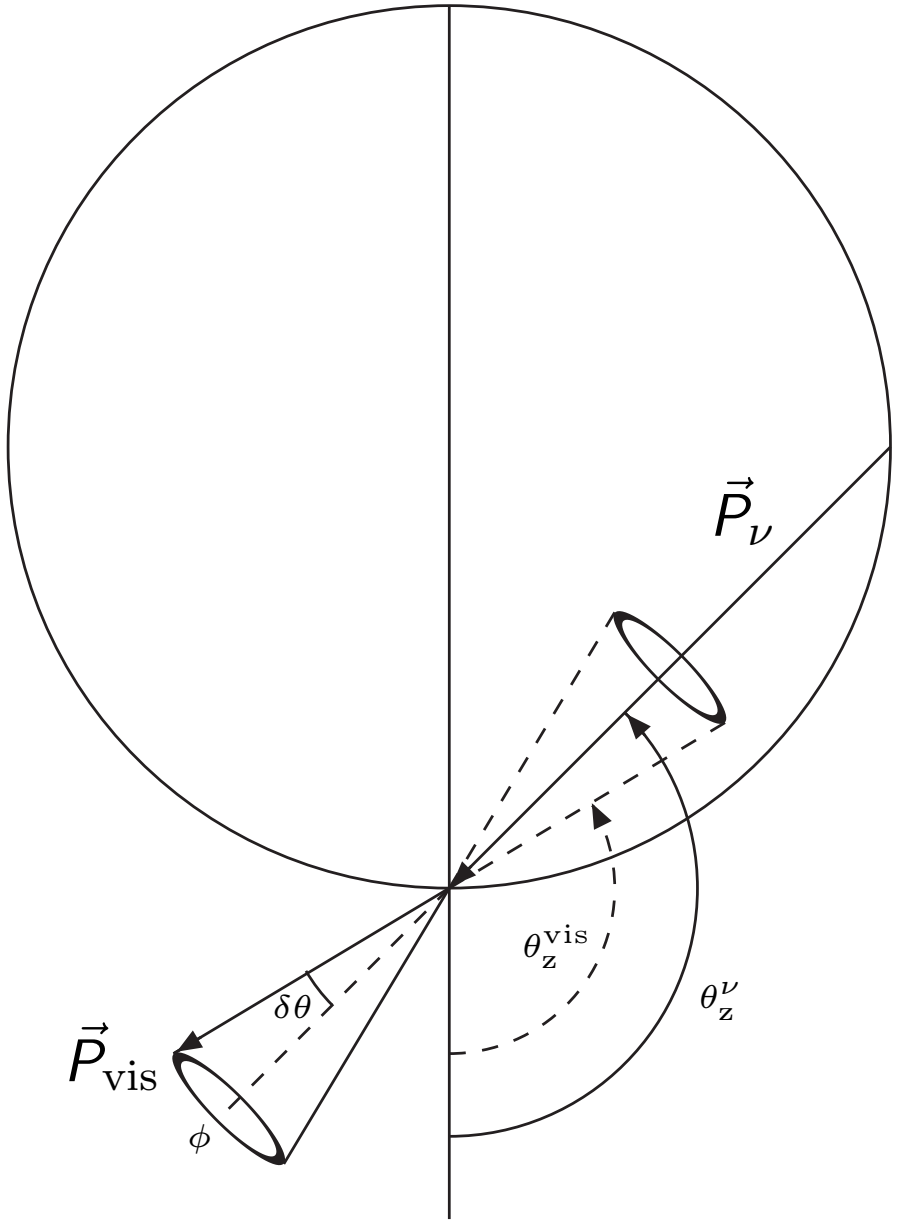

$$\cos\theta_z^{\rm vis} = \cos\theta_z^\nu \cos\delta\theta - \sin\theta_z^\nu \sin\delta\theta \cos\phi\,,$$
$$\min(0, \theta_z^\nu - \delta\theta) \le \theta_z^{\rm vis} \le \max(\pi, \theta_z^\nu + \delta\theta)\,.$$

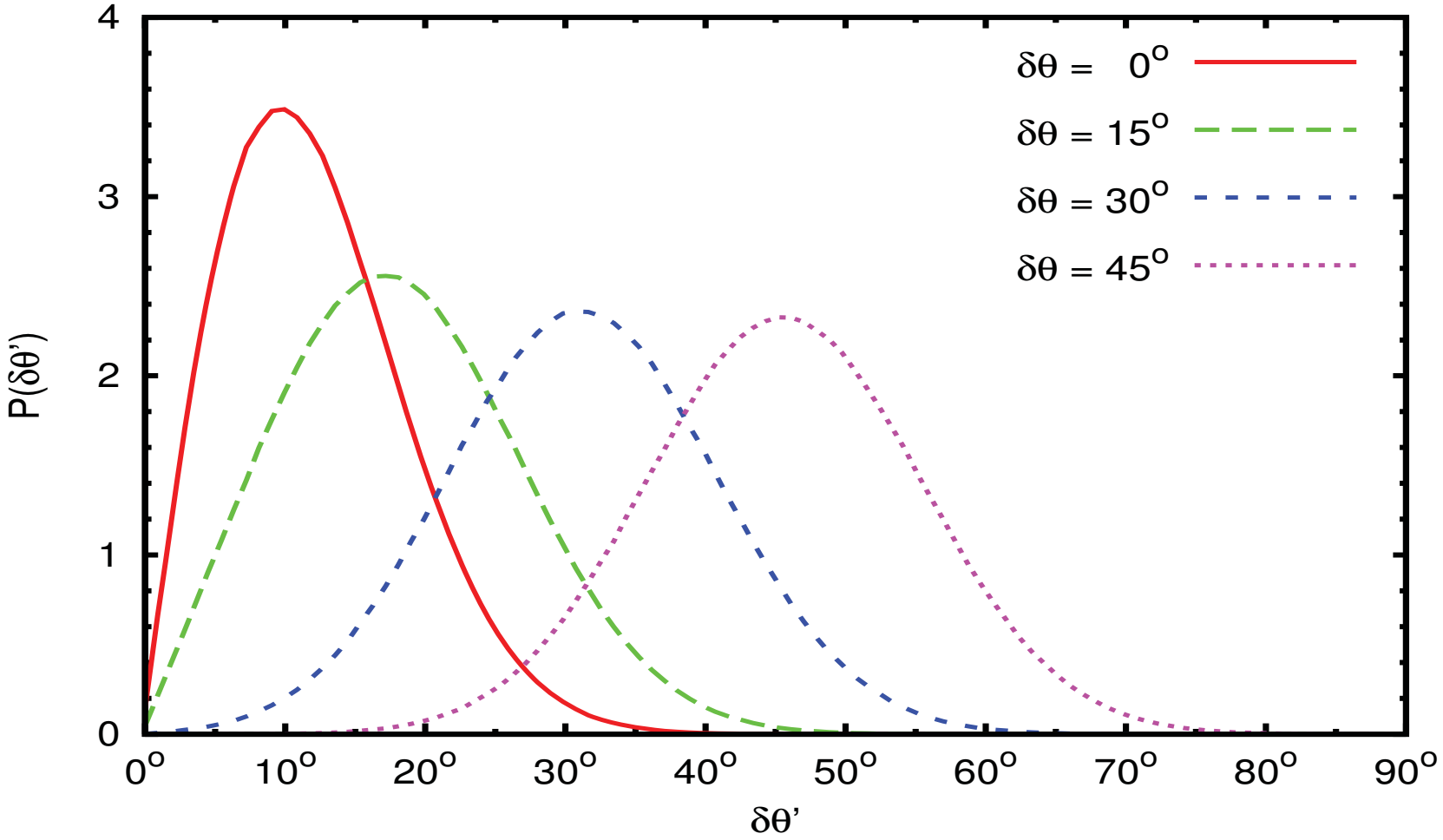

Figure 6. Illustration of transferring angular resolution with $\sigma_\theta = 15^\circ$ from the $\vec{P}_{\rm vis}$ frame to the $\vec{P}_\nu$ frame.

$$\sigma_\theta = \begin{cases} 1.0 \times 15^\circ \times (E_\mu/\mathrm{GeV})^{-0.6}\,, & E_\mu > 1\,\mathrm{GeV}, 1-y_\mu > 0.2 \\ 1.5 \times 15^\circ \times (E_\mu/\mathrm{GeV})^{-0.6}\,, & E_\mu > 1\,\mathrm{GeV}, 1-y_\mu < 0.2 \\ 2.0 \times 15^\circ \times (E_\mathrm{e}/\mathrm{GeV})^{-0.6}\,, & E_\mathrm{e} > 1\,\mathrm{GeV}, 1-y_\mathrm{e} > 0.2 \\ 3.0 \times 15^\circ \times (E_\mathrm{e}/\mathrm{GeV})^{-0.6}\,, & E_\mathrm{e} > 1\,\mathrm{GeV}, 1-y_\mathrm{e} < 0.2 \\ \mathbb{P}(\theta_\mathrm{z}^\ell)|_{E_\ell<1\,\mathrm{GeV}}, & E_\ell < 1\,\mathrm{GeV}, NC, \tau - CC \text{ with } \tau \to \text{hadrons}\,. \end{cases} \tag{4.3}$$

The kinematics of the smearing from angular resolution takes exactly the same form as the kinematics of the smearing from neutrino scattering, shown in figure 3. The only modification is $\vec{P}_\nu \to \vec{P}_\mathrm{vis}$ and $\vec{P}_\mathrm{vis} \to \vec{P}'_\mathrm{vis}$ where P'_vis is the actually measured visible momentum. They can be parametrized as,

$$-\vec{P}_\mathrm{vis} \equiv \left|\vec{P}_\mathrm{vis}\right| \begin{pmatrix} \sin\delta\theta \\ 0 \\ \cos\delta\theta \end{pmatrix}\,, \qquad -\vec{P}'_\mathrm{vis} \equiv \left|\vec{P}'_\mathrm{vis}\right| \begin{pmatrix} \sin\delta\theta'\cos\phi'_\mathrm{vis} \\ \sin\delta\theta'\sin\phi'_\mathrm{vis} \\ \cos\delta\theta' \end{pmatrix}\,, \tag{4.4}$$

in the neutrino frame where $\vec{P}_\nu$ aligns with the z-axis. Note that $\delta\theta$ is the opening angle between $\vec{P}_\nu$ and $\vec{P}_\mathrm{vis}$, determined by the neutrino scattering. Here, the opening angle $\delta\Theta$ between $\vec{P}_\mathrm{vis}$ and $\vec{P}'_\mathrm{vis}$ distributes according to detector resolution,

$$\mathbb{P}(\delta\Theta) = \frac{\sin\delta\Theta}{N(\sigma_\theta)} \exp\left[-\frac{1}{2}\left(\frac{\delta\Theta}{\sigma_\theta}\right)^2\right]\,, \tag{4.5}$$

Detector Performance – Reconstruction & Resolution

- **Energy**
  - $\mathbf{E}_{\rm vis} = \begin{cases} E_\mu + E_{\rm cas} & \mu(E_\mu > 1GeV \ \& \ 1-y \equiv \frac{E_\mu}{E_{\rm vis}} > 0.2) \\ \frac{E_\ell}{0.8} + E_{\rm cas} & \mu(E_\mu < 1GeV \ \text{or} \ 1-y < 0.2), e \ \& \ NC \end{cases}$
  - $\mathbf{\Delta E} = 0.2\sqrt{E}$ for E_ℓ & $E_{\rm cas}(\equiv E_\nu - E_\ell - E_{\nu'})$.
- **Zenith Angle**
  - $\vec{\mathbf{P}}_{\rm vis} = \begin{cases} \vec{P}_\ell, & E_\ell > 1GeV \\ \vec{P}_\nu - \vec{P}_{\nu'}, & E_\ell < 1GeV \ \& \ NC \end{cases} \equiv |P_{\rm vis}| \begin{pmatrix} \sin\theta_\ell \cos\phi_\ell \\ \sin\theta_\ell \sin\phi_\ell \\ \cos\theta_\ell \end{pmatrix}$
  - $\mathbf{\Delta\theta} = \begin{cases} 1.0 \times 15^\circ E_\mu^{-0.6}, & \mu \text{ with } E_\mu > 1GeV, 1-y > 0.2 \\ 1.5 \times 15^\circ E_\mu^{-0.6}, & \mu \text{ with } E_\mu > 1GeV, 1-y < 0.2 \\ 2.0 \times 15^\circ E_e^{-0.6}, & e \text{ with } E_e > 1GeV, 1-y > 0.4 \\ 3.0 \times 15^\circ E_e^{-0.6}, & e \text{ with } E_e > 1GeV, 1-y < 0.4 \\ P(\theta_\ell)|_{E_\ell < 1GeV}, & E_\ell < 1GeV \ \& \ NC \end{cases}$

Enhancing the **MH sensitivity** by splitting the μ events

$$\frac{d\sigma_{\nu}^{CC}}{d(1-y)} = \left[0.72 + 0.06(1-y)^2\right] 10^{-38}\text{cm}^2 \frac{E_\nu}{1GeV}$$

$$\frac{d\sigma_{\bar{\nu}}^{CC}}{d(1-y)} = \left[0.09 + 0.69(1-y)^2\right] 10^{-38}\text{cm}^2 \frac{E_{\bar{\nu}}}{1GeV} \qquad 1303.0758$$

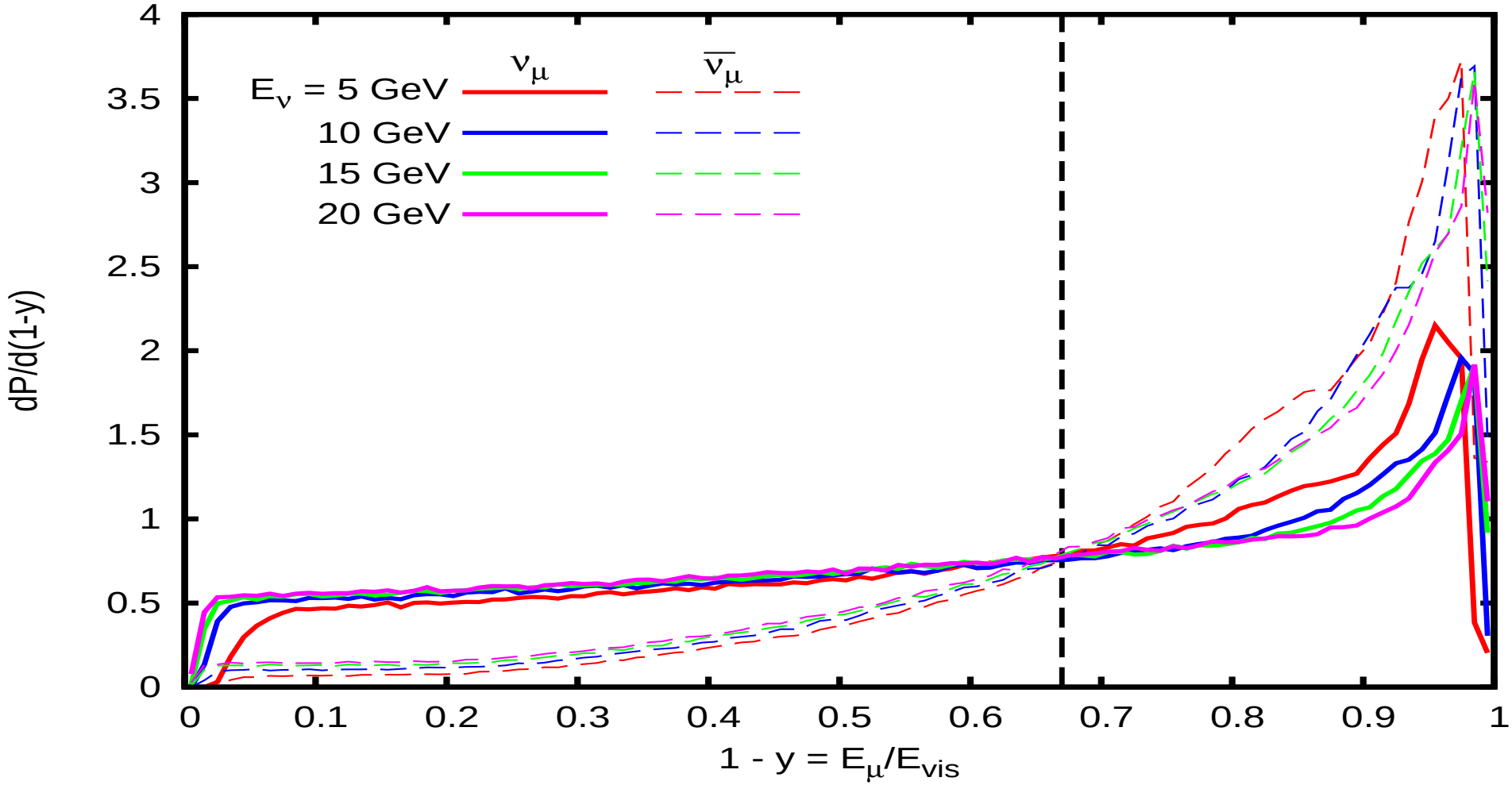

Ability of Distinguishing ν & $\bar{\nu}$

- **HK** 1109.3262
  - μ – NO
  - e (multi-GeV, non-QE) – YES
    - single-ring
      - $\nu_e \to e^- + (\pi^+ \to \mu^+ \to e^+,$ **delayed signal**$)$
      - $\bar{\nu}_e \to e^+ + (\pi^-$ absorbed by water$)$
    - multi-ring
      - ν_e flat distribution of **1-y**
      - $\bar{\nu}_e$ tend to have large **1-y**
- **INO** 1212.1305, 1303.2534, 1306.1423
  - μ – YES, by **Magnetic Field**
  - e – NO
- **Liquid Argon** hep-ph/0510131
  - μ – YES, by **Magnetic Field**
  - e – YES, like HK (?)
- **PINGU** 1205.4965, 1303.0758
  - μ – YES
    - ν_μ flat distribution of **1-y**
    - $\bar{\nu}_\mu$ tend to have large **1-y**
  - e – NO

Events Rates with **Neutrino Scattering**

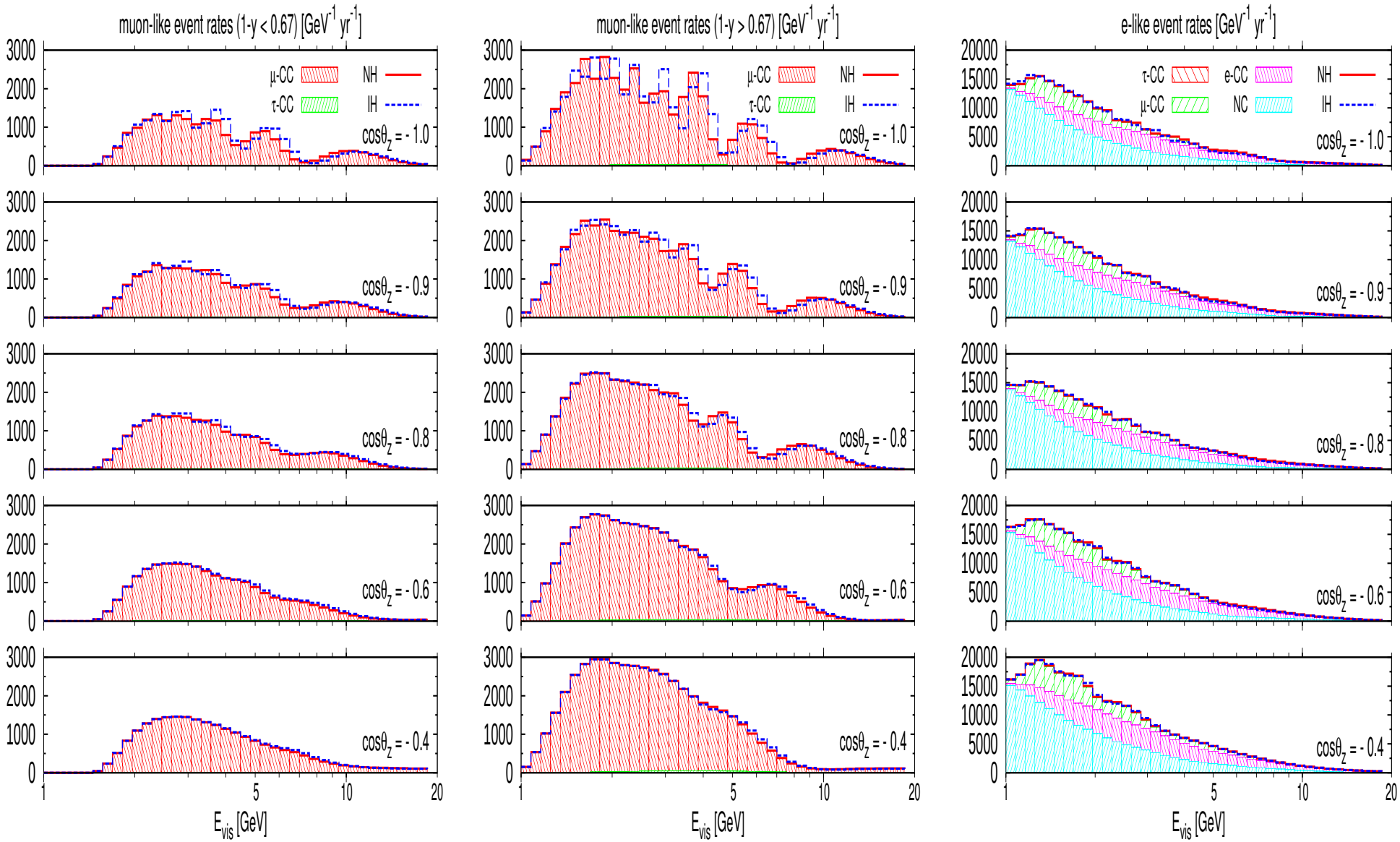

Events Rates with **Detector Resolution** (full Smearing)

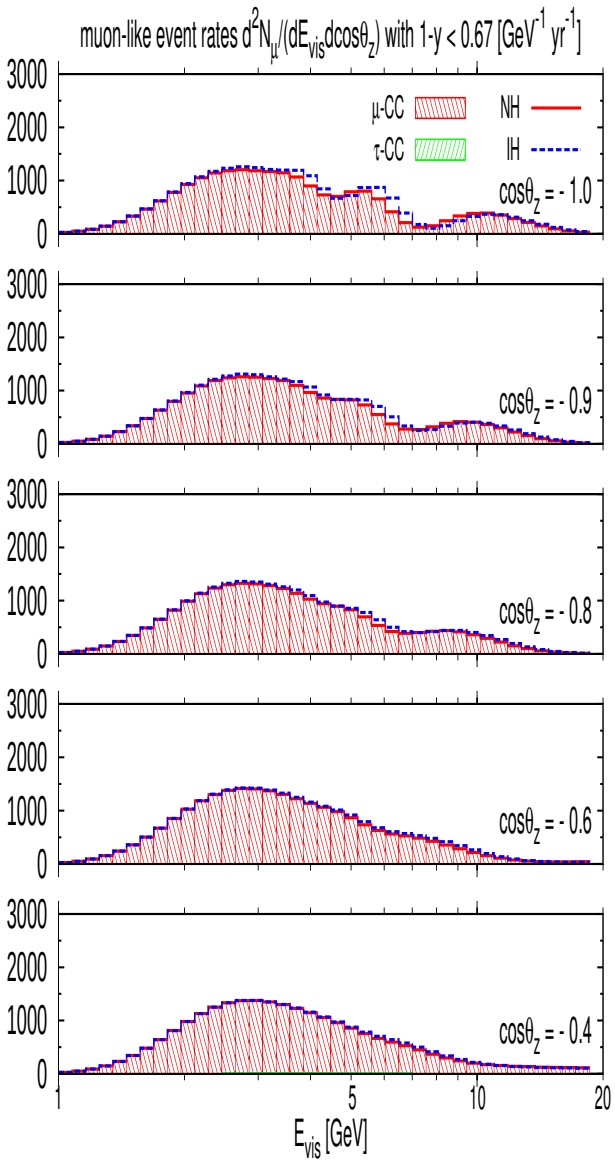

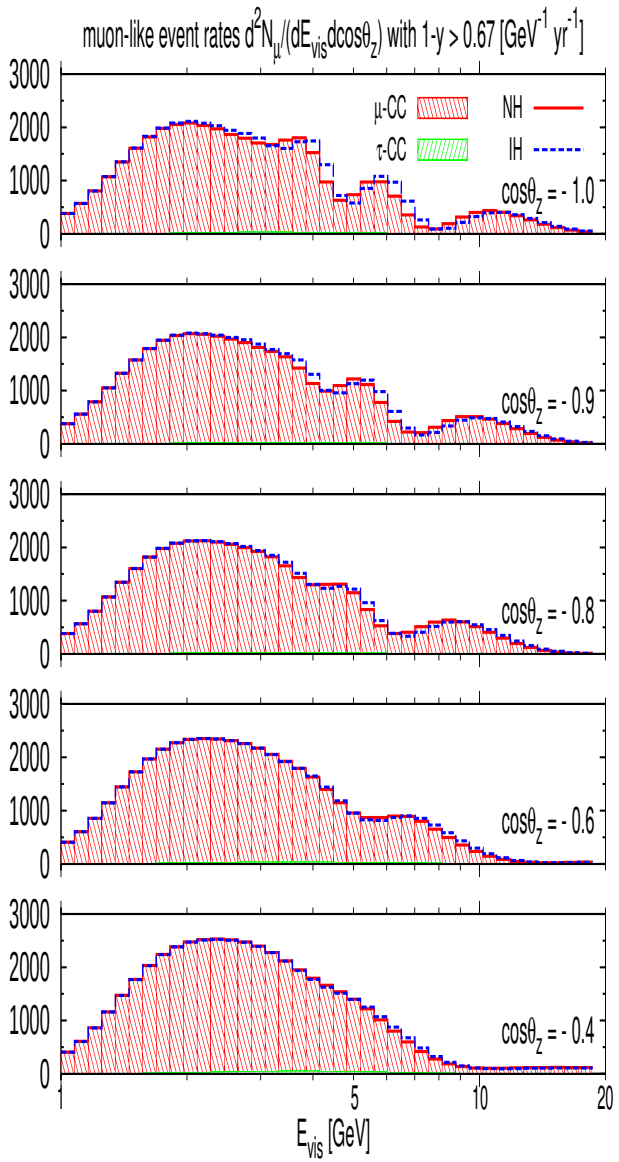

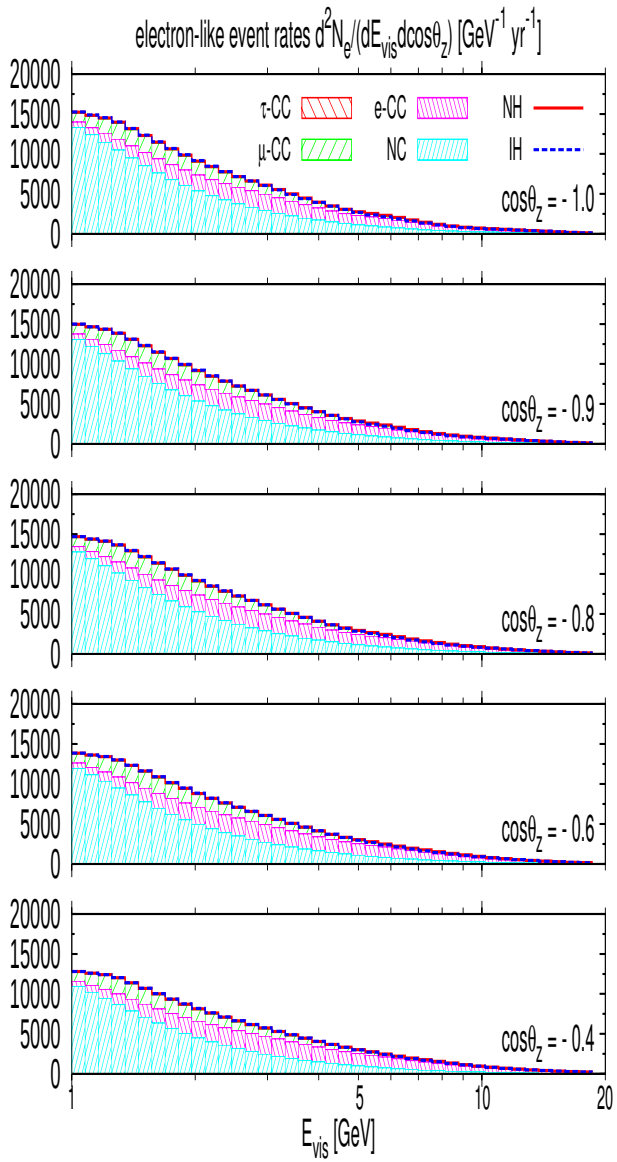

MH Sensitivity Distribution with **Neutrino Scattering**

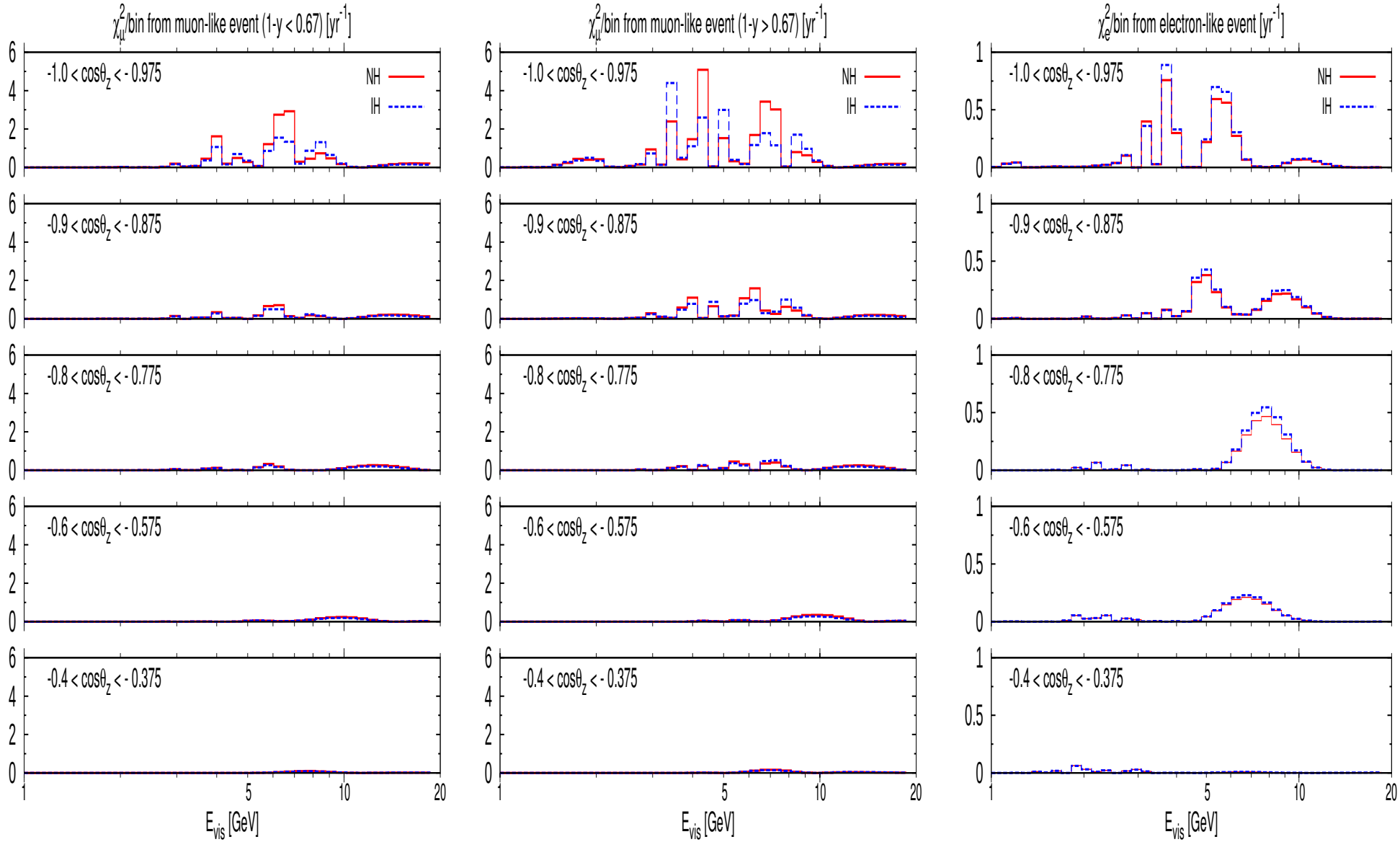

MH Sensitivity Distribution with **Detector Resolution**

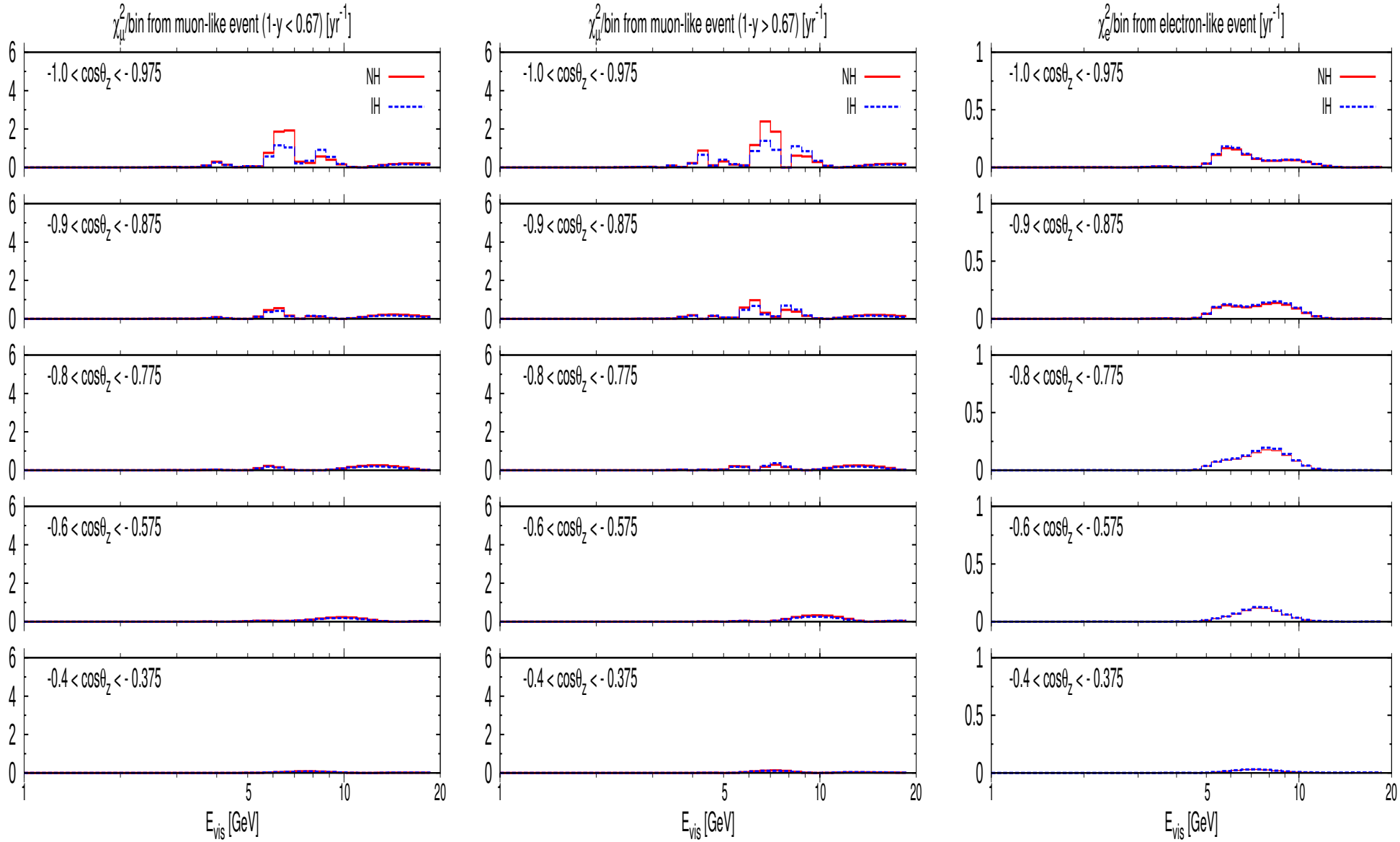

4.3. χ^2 Function

The χ^2 function receives contribution from each E_ν and $\cos\theta_z$ bin as

$$\chi^2 \equiv \sum_\alpha \int dE_\nu d\cos\theta_z \left[\frac{\left(\frac{dN_\alpha}{dE_\nu d\cos\theta_z}\right)^{th} - \left(\frac{dN_\alpha}{dE_\nu d\cos\theta_z}\right)^{obs}}{\sqrt{\left(\frac{dN_\alpha}{dE_\nu d\cos\theta_z}\right)^{obs}}} \right]^2 + \chi^2_{para}\,, \tag{4.5}$$

where χ^2_{para} is the contribution from parameters,

$$\begin{aligned} \chi^2_{para} &= \left[\frac{(\delta m^2_a)^{fit} - \delta m^2_a}{\Delta\delta m^2_a}\right]^2 + \left[\frac{(\delta m^2_s)^{fit} - \delta m^2_s}{\Delta\delta m^2_s}\right]^2 \\ &+ \left[\frac{(\sin^2 2\theta_r)^{fit} - \sin^2 2\theta_r}{\Delta \sin^2 2\theta_r}\right]^2 + \left[\frac{(\sin^2 2\theta_s)^{fit} - \sin^2 2\theta_s}{\Delta \sin^2 2\theta_s}\right]^2 + \left[\frac{(\sin^2 2\theta_a)^{fit} - \sin^2 2\theta_a}{\Delta \sin^2 2\theta_a}\right]^2, \end{aligned} \tag{4.6}$$

with the current central values and expected uncertainties in the near future [41, 42, 43],

$$\delta m^2_a = 2.35 \pm 0.1 \times 10^{-3}\mathrm{eV}^2\,, \qquad \delta m^2_s = 7.50 \pm 0.2 \times 10^{-5}\mathrm{eV}^2\,, \qquad \sin^2 2\theta_s = 0.857 \pm 0.024\,, \tag{4.7a}$$

$$\sin^2 2\theta_r = 0.098 \pm 0.005\,, \qquad \sin^2 2\theta_a = 0.957 \pm 0.030\,, \tag{4.7b}$$

MH Sensitivity with μ or μ+e ($E > 4GeV$ & $\cos\theta_z < -0.4$) ▸ Rates

$\Delta\chi^2_{\rm MH}$	NH (true)			IH (true)		
$\bar{x}_a$ (true)	-0.2	0	$+0.2$	-0.2	0	$+0.2$
ν	163.0 252.9	174.9 215.3	141.8 168.9	100.7 143.5	109.7 140.7	96.7 120.1
Scattering	26.4 67.3	13.2 32.2	10.2 21.3	14.9 21.2	12.7 17.9	10.1 15.4
Resolution	22.9 44.1	10.2 17.4	7.1 9.2	9.9 14.8	8.7 13.8	7.0 10.0
μ mis-ID	20.8 40.5	9.3 16.0	6.5 8.5	9.1 14.0	8.0 12.9	6.4 9.3
Split μ ($1 - y \gtrless 0.67$)	27.1 46.9	12.6 19.5	8.1 9.9	12.8 16.8	10.9 15.9	7.9 10.8
$\sigma_E = (0.2 \pm 0.03) \times \sqrt{E}$	26.1 42.3	11.2 18.0	7.7 8.6	11.5 16.0	10.0 14.8	7.1 9.9
$\sigma_\theta = (15^\circ \pm 3^\circ) \times E^{-0.6}$	26.3 43.1	11.5 18.2	7.9 9.0	11.8 16.1	9.9 15.1	7.6 10.0
μ mis-ID ($10\% \pm 2\%$)	19.0 42.1	8.4 17.1	6.1 8.5	8.8 15.3	7.2 13.3	5.3 9.2
Normalization (1 ± 0.05)	16.8 43.6	7.9 16.9	6.6 8.7	8.6 14.0	6.9 13.8	5.0 8.7
Combined	12.6 41.6	7.5 16.1	5.9 8.3	7.5 13.7	6.2 12.2	4.8 7.7

$\mathbf{x_a}$ Uncertainty with μ or μ+e ($E > 4GeV$ & $\cos\theta_z < -0.4$)

$\Delta(x_a)$	NH (true)			IH (true)		
$\bar{x}_a$ (true)	-0.2	0	$+0.2$	-0.2	0	$+0.2$
ν	0.014 0.012	0.036 0.025	0.011 0.010	0.014 0.012	0.046 0.035	0.011 0.011
Scattering	0.025 0.020	0.051 0.039	0.015 0.014	0.024 0.022	0.073 0.061	0.017 0.016
Resolution	0.027 0.021	0.055 0.043	0.016 0.016	0.025 0.024	0.077 0.067	0.018 0.018
μ mis-ID	0.028 0.022	0.059 0.045	0.017 0.017	0.026 0.025	0.078 0.070	0.019 0.019
Split μ ($1 - y \gtrless 0.67$)	0.027 0.022	0.057 0.045	0.017 0.016	0.026 0.024	0.077 0.068	0.019 0.019
$\sigma_E = (0.2 \pm 0.03) \times \sqrt{E}$	0.027 0.025	0.057 0.045	0.017 0.016	0.026 0.025	0.077 0.068	0.019 0.019
$\sigma_\theta = (15^\circ \pm 3^\circ) \times E^{-0.6}$	0.028 0.023	0.057 0.045	0.017 0.017	0.026 0.024	0.078 0.069	0.019 0.019
μ mis-ID ($10\% \pm 2\%$)	0.028 0.022	0.069 0.052	0.021 0.020	0.028 0.026	0.083 0.078	0.024 0.020
Normalization (1 ± 0.05)	0.033 0.023	0.081 0.055	0.025 0.022	0.031 0.027	0.090 0.078	0.030 0.021
Combined	0.034 0.026	0.083 0.058	0.028 0.024	0.033 0.029	0.099 0.081	0.032 0.023

Octant Sensitivity with μ or μ+e ($E > 4GeV$ & $\cos\theta_z < -0.4$)

$\Delta\chi^2_{\text{Octant}}$	NH (true)				IH (true)			
$\bar{x}_a$ (true)	-0.2	-0.1	$+0.1$	$+0.2$	-0.2	-0.1	$+0.1$	$+0.2$
ν	41.5 84.8	6.7 15.1	20.6 29.3	64.1 162.6	10.3 32.5	2.9 8.0	4.1 12.0	12.9 46.0
Scattering	24.4 36.9	3.1 6.2	9.6 13.2	47.7 103.0	7.5 15.6	1.8 3.3	2.8 5.5	9.9 21.4
Resolution	20.4 27.9	2.6 4.4	8.3 10.2	43.4 76.2	6.3 11.1	1.4 2.3	2.5 4.1	8.8 15.4
μ mis-ID	18.6 25.9	2.4 4.1	7.5 9.2	39.2 69.9	5.7 10.3	1.3 2.1	2.2 3.7	7.9 14.3
Split μ ($1 - y \gtrless 0.67$)	19.6 26.9	2.5 4.2	7.8 9.5	40.4 70.9	6.6 11.2	1.5 2.3	2.5 4.0	8.7 15.1
$\sigma_E = (0.2 \pm 0.03) \times \sqrt{E}$	19.4 26.3	2.5 4.1	7.7 9.1	40.0 65.8	6.5 10.8	1.5 2.3	2.5 3.8	8.7 14.3
$\sigma_\theta = (15^\circ \pm 3^\circ) \times E^{-0.6}$	19.3 26.7	2.5 4.2	7.7 9.1	40.2 66.8	6.6 11.0	1.5 2.3	2.5 3.8	8.7 14.5
μ mis-ID ($10\% \pm 2\%$)	19.1 26.5	2.2 4.0	5.2 8.2	39.2 66.1	4.5 10.8	1.3 2.0	1.9 2.7	8.3 13.8
Normalization (1 ± 0.05)	10.5 26.5	1.8 4.2	3.1 9.2	13.1 70.6	3.5 11.1	0.9 2.1	0.9 3.7	3.6 14.8
Combined	9.3 20.0	1.7 3.2	2.8 7.6	12.4 33.9	3.4 8.6	0.8 1.9	0.8 1.9	3.5 9.1

Conclusions:

- Atmospheric neutrinos produced in the other side of the earth can be studied in detail at a huge underground detector such as **PINGU** in ICECUBE , which can
  (1) determine the mass hierarchy
  (2) resolve the octant $x_a = \cos^2\theta_{23} - \sin^2\theta_{23} > 0$ vs < 0
  (3) but to measure $\delta_{\rm MNS}$ may be challenging.

- By adopting the Propagation Basis the earth matter effects can be treated efficiently, exactly and systematically, allowing us to perform the full parameter scan including systematic uncertainties.

- By defining our estimates for the neutrino energy E_ν and its momentum direction θ_ν for all types of events (CC, NC and τ events), we should treat the neutrino scattering effects exactly by using event generators, such as Genie, Nuance, Neut, etc.

- Finite resolution of the detector can then be studied quantitatively for E_ν and θ_ν, which depend on the type of neutrino interactions.

Conclusions (continued):

- We study the following systematic effects:

  (1) 15% error in $0.2/\sqrt{E_\nu}$ resolution of E_ν
  (2) 20% error in $15^\circ/E^{-0.6}$ resolution of θ_ν
  (3) 20% error in μ-miss ID probability of 0.1
  (4) 5% error in the overall normalization of flux $\times\sigma_\nu$

  and find that our conclusions hold even after all the four uncertainties are simultaneously taken account of.

- After all the above systematic uncertainties are accounted for, our full parameter scan (within the 3-neutrino model) gives:

  (1) The neutrino **mass hierarchy** can be determined with **6, 4, 3**σ for $x_a = -0.2$, 0, 0.2, for NH, and with **3.7, 3.5, 2.8**σ for IH.
  (2) The error of $x_a = \cos^2\theta_{23} - \sin^2\theta_{23}$ is 0.026, 0.058, 0.024 for $x_a = -0.2$, 0, 0.2, for NH, while it is 0.029, 0.081, 0.023 for IH.
  (3) The **octant** ($x_a > 0 (\theta_{23} < \pi/4)$ **or** $x_a < 0 (\theta_{23} > \pi/4)$) can be resolved with **4.5, 5.8**σ for $x_a = -0.2$, 0.2 for NH, and with **2.9, 3.0**σ for IH.
  (4) No appreciable sensitivity to the CP phase δ_{MNS} is found.

  after **1 year running of PINGU**.